The Reaction of 5,10,15,20-Tetrakis(2,6-dichloro-3-sulfonatophenyl)porphinatoiron(III) Hydrate with Alkyl and Acyl Hydroperoxides. The Dynamics of Reaction of Water-Soluble and Non μ-Oxo Dimer Forming Iron(III) Porphyrins in Aqueous Solution. 7

Kazuhisa Murata, Rick Panicucci, Enona Gopinath, and Thomas C. Bruice*

Contribution from the Department of Chemistry, University of California at Santa Barbara, Santa Barbara, California 93106. *Received December 15, 1989*

Abstract: Kinetic and product studies (30 °C, μ = 0.20 with $NaNO_3$, between pH 1.0 and 12.35) are reported for the reaction in water of an iron(III) octa-*o*-chloro-substituted tetraphenylporphyrin [5,10,15,20-tetrakis(2,6-dichloro-3-sulfonatophenyl)porphinatoiron(III) hydrate ((**2**)$Fe^{III}(H_2O)_2 \rightleftharpoons$ (**2**)$Fe^{III}(HO)(H_2O) + H^+ \rightleftharpoons$ (**2**)$Fe^{III}(OH)_2 + 2H^+$) with a number of acyl and alkyl hydroperoxides (*t*-BuOOH, $Ph(CH_3)_2COOH$, $Ph_2(CO_2CH_3)COOH$, $Ph_2(CN)COOH$, *m*-$ClC_6H_4CO_3H$, *p*-$NO_2C_6H_4CO_3H$, and $PhCH_2CO_3H$). All reactions are first-order in the hydroperoxide and in (**2**)$Fe^{III}(X)_2$ (where X = H_2O, HO^-). The rates are (1) insensitive to the presence or absence of O_2 and (2) not subject to specific-acid, general-acid, nor general-base catalysis at any pH. For the reaction with *t*-BuOOH, characteristics of the pH dependence of the second-order rate constant (k_{1y}) are as follows: (1) < pH 3.5, k_{1y} is pH independent; (2) from pH 3.5 to 9.5, k_{1y} increases and then decreases ("bell-shape curve"); (3) above pH 10, k_{1y} again increases and then decreases (second "bell-shape curve"). These results are explained if one assumes that three steady-state intermediates [(**2**)$Fe^{III}(H_2O)$(*t*-BuOOH), (**2**)$Fe^{III}(HO^-)$(*t*-BuOOH) $\rightleftharpoons$ (**2**)$Fe^{III}(H_2O)$(*t*-$BuOO^-$), and (**2**)$Fe^{III}(HO^-)$(*t*-$BuOO^-$)] break down in the commitment step and are in acid–base equilibria. From product analysis, reactions with *t*-BuOOH provide 90% yield of $(CH_3)_2CO$ and >50% yield of CH_3OH. Neither CH_4, C_2H_6, O_2, or $(t\text{-BuO})_2$ could be detected. In the presence of 2,2′-azinobis(3-ethylbenzthiazoline-6-sulfonate) (ABTS) trap, $(CH_3)_2CO$ is formed in 10–20% yield, and the main product (80–90%) is *t*-BuOH. With $Ph(CH_3)_2COOH$, $Ph(CH_3)C{=}O$ was formed in ~70% yield at pH 7.25. Neither PhOH nor $(CH_3)_2C{=}O$ could be detected. These findings uniquely identify $R(CH_3)_2CO^\bullet$ intermediates and allow the mechanism (**2**)$Fe^{III}(H_2O)(X) + R(CH_3)_2COOH \rightarrow$ /(**2**)$Fe^{IV}(O)(X) + R(CH_3)_2CO^\bullet$/ $\rightarrow$ (**2**)$Fe^{IV}(O)(X) + R(CH_3)_2CO^\bullet$ followed by fragmentation of $R(CH_3)_2CO^\bullet$ (within the /intimate pair/ and after solvent separation) to provide $R(CH_3)C{=}O + CH_3^\bullet$. Reaction of $CH_3^\bullet$ with (**2**)$Fe^{III}(H_2O)(X)$ or (**2**)$Fe^{IV}(O)(X)$ leads to CH_3OH plus (**2**)$Fe^{II}(H_2O)$ and (**2**)$Fe^{III}(H_2O)(X)$, respectively. The putative (**2**)$Fe^{II}(H_2O)$ species was trapped (20% yield) with CO as (**2**)$Fe^{II}(CO)$. The difference in product yields in the presence and absence of ABTS may be explained by the inability of ABTS to trap the components of the initially formed solvent caged pair, /(**2**)$Fe^{IV}(O)(X) + R(CH_3)_2CO^\bullet$/, but essentially complete trapping of the solvent-separated (**2**)$Fe^{IV}(O)(X)$ and $R(CH_3)_2CO^\bullet$ species. The reaction of (**2**)$Fe^{III}(X)_2$ with *t*-BuOOH, and the other alkyl and acyl hydroperoxides investigated, gives rise to an observable iron(IV)-oxo porphyrin intermediate between pH 2.0 and 12. The formation of (**2**)$Fe^{IV}(O)(X)$ with *t*-BuOOH or $Ph(CH_3)_2COOH$ requires the presence of O_2. This is consistent with the formation of (**2**)$Fe^{IV}(O)(X)$ from the reaction of (**2**)$Fe^{II}(H_2O)$ with O_2. Once generated, the spectra of the (**2**)$Fe^{IV}(O)(X)$ species persist for an extended time [70 h (pH 4.87), 100 h (pH 6.3), 80 h (pH 7.25), 50 h (pH 10.37), and 24 h (pH 11.68)] prior to reconversion (>95%) to (**2**)$Fe^{III}(H_2O)(X)$. Thus octa-*o*-chloro substitution provides greater stabilization of the iron(IV)-oxo tetraphenylporphyrin as compared to octa-*o*-methyl substitution. (**2**)$Fe^{IV}(O)(X)$ is formed even in the absence of O_2 in the reaction of (**2**)$Fe^{III}(H_2O)(X)$ with acyl hydroperoxides (*p*-$NO_2C_6H_4CO_3H$, *m*-$ClC_6H_4CO_3H$ and $PhCH_2CO_3H$) and with alkyl hydroperoxides ($Ph_2(CN)COOH$ and $Ph_2(CO_2CH_3)COOH$). The reaction of H_2O_2 with (**2**)$Fe^{III}(H_2O)(X)$ does not generate (**2**)$Fe^{IV}(O)(X)$, and a rapid decomposition of (**2**)$Fe^{III}(H_2O)(X)$ occurs. Hydrogen peroxide reacts rapidly with authentic (**2**)$Fe^{IV}(O)(X)$.

Introduction

The reactions of metalloporphyrins with oxidizing agents such as iodosylbenzene, peracids, and hydroperoxides have been used to model the chemistry of hemeproteins such as cytochrome P-450, catalase, and peroxidases. The nature and structure of the intermediates generated from these reactions are of great interest. It is generally accepted that reactions with iodosylbenzene and peracids (eq 1) result in the formation of an iron(IV)-oxo porphyrin π-cation radical.[1] The transfer of the oxygen atom in eq 1 has been shown to occur by heterolytic O–O bond cleavage, and

$$[(porph)Fe^{III}]^+ + RCO_3H \rightarrow [(porph^{\bullet+})Fe^{IV}{=}O]^+ + RCO_2H \quad (1)$$

the intermediate is capable of stereospecific olefin epoxidation. The reaction of hydroperoxides with iron(III) porphyrins is more biologically relevant and has drawn particular attention. A number of studies have provided evidence for the homolytic scission of the O–O bond to provide an iron(IV)-oxo species (eq 2).[2] Other

$$[(porph)Fe^{III}]^+ + ROOH \rightarrow [(porph)Fe^{IV}{=}O] + RO^\bullet + H^+ \quad (2)$$

product and kinetic studies have been offered in support of O–O bond heterolysis.[3a,b] These investigations have employed, in the main, 5,10,15,20-tetrakis(2,6-dichlorophenyl)porphinatoiron(III)

(1) (a) Groves, J. T.; Nemo, T. E.; Meyers, R. S. *J. Am. Chem. Soc.* **1979**, *101*, 1032. (b) Groves, J. T.; Haushalter, R. C.; Nakamura, M.; Nemo, T. E.; Evans, B. J. *J. Am. Chem. Soc.* **1981**, *103*, 2884. (c) Groves, J. T.; Watanabe, Y. *J. Am. Chem. Soc.* **1988**, *110*, 8443. (d) Lee, W. A.; Bruice, T. C. *J. Am. Chem. Soc.* **1985**, *107*, 513. (e) Lee, W. A.; Yuan, L. C.; Bruice, T. C. *J. Am. Chem. Soc.* **1988**, *110*, 4277.

(2) (a) Balasubramanian, P. N.; Lee, R. W.; Bruice, T. C. *J. Am. Chem. Soc.* **1989**, *111*, 8714. (b) Bruice, T. C.; Balasubramanian, P. N.; Lee, R. W.; Lindsay Smith, J. R. *J. Am. Chem. Soc.* **1988**, *110*, 7890. (c) Lindsay Smith, J. R.; Balasubramanian, P. N.; Bruice, T. C. *J. Am. Chem. Soc.* **1988**, *110*, 7411. (d) Balasubramanian, P. N.; Lindsay Smith, J. R.; Davies, M. J.; Kaaret, T. W.; Bruice, T. C. *J. Am. Chem. Soc.* **1989**, *111*, 1477. (e) Arasasingham, R. D.; Cornman, C. R.; Balch, A. L. *J. Am. Chem. Soc.* **1989**, *111*, 7800. (f) Labeque, R.; Marnett, L. J. *J. Am. Chem. Soc.* **1989**, *111*, 6621. (g) Mansuy, D.; Bartoli, J. F.; Mometeau, M. *Tetrahedron Lett.* **1982**, *23*, 2781. (h) Castellino, A.; Bruice, T. C. *J. Am. Chem. Soc.* **1988**, *110*, 158.

(3) (a) Traylor, T. G.; Fann, W. D.; Bandyopadhyay, D. *J. Am. Chem. Soc.* **1989**, *111*, 8009. (b) Traylor, T. G.; Ciccone, J. P. *J. Am. Chem. Soc.* **1989**, *111*, 8413.

0002-7863/90/1512-6072$02.50/0

salts [$(Cl_8TPP)Fe^{III}(Cl)$] as the catalyst. Kinetic evidence offered in support of heterolytic O–O bond scission with hydroperoxides[3b] revolves around the detection of general-acid catalysis. The following comments can be made. There is no evidence that general-acid catalysis is associated with heterolytic O–O bond scission of hydroperoxides. In regards to the kinetic studies offered in support of heterolysis, the experimental protocols used in these investigations deviate severely from accepted practices for solution kinetics[5] and are conducted in such a manner as to render them inconclusive, specifically: (1) Rate constants in MeOH solvent were determined under conditions where the ionic strength varied by as much as ~0–0.5, and (2) in some cases buffering was not employed. Also, (3) acidity dependent reactions were studied without the measurement of pH; instead, the pH was calculated from pK_a's of buffer substances used. However, these pK_a's are variable and depend on the ionic strength of the solution, which was unknown. Furthermore, (4) the pK_a value of methanol ligated iron(III) porphyrin was not taken into account. Therefore, the enhancement of rate on increase in total buffer concentration cannot be attributed to either general-acid or general-base catalysis. In regards to the use of derived rate constants (k_r) in linear-free energy plots of log k_r vs pK_a of leaving alcohol the calculated pK_a values[3b] for the alcohols $Ph_2(COOCH_3)COH$ (pK_a 12.8) and $Ph_2(CN)COH$ (10.7) appear to be in error. We find the pK_a values to be 11.1 for $Ph_2(COOCH_3)COH$ and 9.1 for $Ph_2(CN)COH$ [by the methods of Charton[6a] and Fox and Jencks[6b] using the pK_a of MeOH (15.5)[6c] along with ρ_I (−8.2 to −8.4) and σ_I values (−Ph, 0.1; −CN, 0.56; $-CO_2Me$, 0.34)].

Alkene epoxidation was reported at high concentrations of $(Cl_8TPP)Fe^{III}(X)$ with *t*-BuOOH or H_2O_2 at 0.2 M and norbornene at 1.0 M in a solvent composed of $CH_2Cl_2/CH_3OH/H_2O$ = 59.3:39.3:1.4.[3a] This is an important observation. We have repeated this experiment and concur with the observations. Interpretation of the results can be as follows: (i) epoxide is a primary product from reaction of alkene with $(^{+\bullet}Cl_8TPP)Fe^{IV}(O)$, which would implicate heterolytic cleavage of the O–O bonds of the hydroperoxides as proposed[3a]; (ii) rate controlling homolytic O–O bond cleavage and indirect formation of $(^{+\bullet}Cl_8TPP)Fe^{IV}(O)$; and (iii) epoxidation by other[2f] than $(^{+\bullet}Cl_8TPP)Fe^{IV}(O)$.

Concerning (ii), one possibility for indirect formation of $(^{+\bullet}Cl_8TPP)Fe^{IV}(O)$ is as shown in eq 3. The potential (SCE) for 1e⁻ oxidation of $(Cl_8TPP)Fe^{IV}(O)$ to $(^{+\bullet}Cl_8TPP)Fe^{IV}(O)$ is 1.2

$$[(Cl_8TPP)Fe^{III}]^+ + H_2O_2 \rightarrow (Cl_8TPP)Fe^{IV}(O) + {}^{\bullet}OH \quad (3a)$$

$$(Cl_8TPP)Fe^{IV}(O) + {}^{\bullet}OH \rightarrow (^{+\bullet}Cl_8TPP)Fe^{IV}(O) + HO^- \quad (3b)$$

V (in water[4a]), while the potential for oxidation of HO^- to $HO^{\bullet}$ is 1.65 V (in water[4b]) such that the reaction of eq 3b is favored. The potentials for oxidation of alkyl–O^- to alkyl–$O^{\bullet}$ species are about 0.6 V less positive than for the oxidation of HO^-; however, at high concentrations of alkyl–$O^{\bullet}$ some portion of $(Cl_8TPP)Fe^{IV}(O)$ could be converted to $(^{+\bullet}Cl_8TPP)Fe^{IV}(O)$. Epoxidation is not observed at lower concentrations of reactants.[2a]

Concerning (iii), Labeque and Marnett[2f] have shown, under the same solvent conditions used by Traylor and co-workers,[3a] that *cis*-stilbene is epoxidized by *t*-BuOOH + iron(III) porphyrin to provide both *cis*- and *trans*-stilbene oxides. Since $(^{+\bullet}Cl_8TPP)Fe^{IV}(O)$ species stereospecifically epoxidize *cis*-stilbene to *cis*-stilbene oxide,[2h] the oxidant when using *t*-BuOOH must not be $(^{+\bullet}Cl_8TPP)Fe^{IV}(O)$. It was proposed that the epoxidant with alkyl hydroperoxides and iron(III) porphyrin is $ROO^{\bullet}$.[2f]

Because $(Cl_8TPP)Fe^{III}(X)$ has received considerable attention, and since it is of paramount importance to transfer kinetic studies to aqueous solution, we have investigated the reactions of 5,10,15,20-tetrakis(2,6-dichloro-3-sulfonatophenyl)porphinatoiron(III) hydrate ($(2)Fe^{III}(X)_2$ (X = H_2O or HO^-)) with the YOOH species *t*-BuOOH, $Ph(CH_3)_2COOH$, $Ph_2(COOCH_3)COOH$, $Ph_2(CN)COOH$, *m*-$ClC_6H_4CO_3H$, *p*-$NO_2C_6H_4CO_3H$, and $PhCH_2CO_3H$ in water. In the present study particular attention is given to the following: (i) the pH dependence of the rate for oxidative oxygen transfer using *t*-BuOOH and the nature of products and their yields with *t*-BuOOH and $Ph(CH_3)_2COOH$ in the presence and absence of the 1e⁻ oxidizable trapping agent 2,2'-azinobis(3-ethylbenzthiazoline-6-sulfonate) (ABTS); (ii) the influence of general-acid and general-base species upon the rate; and (iii) the formation of iron(II) and iron(IV) porphyrin intermediate species. With *t*-BuOOH and $Ph(CH_3)_2COOH$, all results are consistent with a mechanism which involves homolytic O–O bond breaking in the *rate-determining* step.

Experimental Section

Almost all the instrumental procedures, materials, and methodologies have been reported previously.[2a-c]

Materials. Deionized, doubly distilled water was used for all experiments. All the buffer and salt solutions were prepared from reagent grade chemicals and passed over a chelex 100 column or were extracted with 0.01% dithiazone in dichloromethane (below pH 6) to remove any heavy metal contamination. Carbon monoxide (Linde, Technical grade) and sodium dithionite (Aldrich Chemical Co.) were used as received. *t*-BuOOH (8.3 M) and $Ph(CH_3)_2COOH$ (95%) were purchased from Aldrich and Sigma, respectively. Ammonium acetate and ammonium sulfate were also commercially available. *m*-Chloroperbenzoic acid and *p*-nitroperbenzoic acid were purchased from Aldrich Chemical Co. Phenylperacetic acid, diphenylcyanomethyl hydroperoxide, and carbomethoxy diphenylmethyl hydroperoxide were from a previous study.[2a]

5,10,15,20-Tetrakis(2,6-dichloro-3-sulfonatophenyl)porphyriniron(III) hydrate $(2)Fe^{III}(H_2O)(X)$ was from the previous study.[7]

Methods. HPLC analyses were carried out with a reverse-phase column (Alltech/Applied Science 250 × 4.6 mm column packed with Lichrosorb RP-18 5 μm) using $MeOH/H_2O$ (50% v/v) mixtures.

Reactions were carried out at 30 °C at μ = 0.2 (with $NaNO_3$). Rapid reactions were followed by use of either a Durrum stopped-flow spectrophotometer or rapid-scan stopped-flow spectrophotometer by using the Harrick monochrometer (Harrick Scientific, Ossining, NY) interfaced to a computer equipped with OLIS data acquisition and processing software.

Experiments with carbon monoxide were carried out inside a N_2 filled glovebox which housed the spectrophotometer. The spectrum of $(2)Fe^{II}(H_2O)(CO)$ was determined by making solutions of $(2)Fe^{III}(H_2O)(X)$ (5.06×10^{-6} M), at pH 7.25 (0.5 M phosphate buffer), in sodium dithionite (1 mM) and then saturating the solution with CO, when formation of $(2)Fe^{II}(H_2O)(CO)$ is complete.[8] In another experiment, a buffered solution (pH 7.25) of $(2)Fe^{III}(H_2O)(X)$ was saturated with CO, *t*-BuOOH was then added (to 1.1×10^{-5} M), and the reaction was followed by visible spectral repetitive scanning.

Results

The reactions of alkyl and acyl hydroperoxides with $(2)Fe^{III}(H_2O)(X)$, where X = H_2O or HO^-, were followed in the presence and absence of 2,2'-azinobis(3-ethylbenzthiazolinesulfonic acid) (ABTS) as a 1e⁻ oxidizable trap for products which are oxidants [pH 1–12.35 in water, μ = 0.20 (with $NaNO_3$), 30 °C]. One-electron oxidation of ABTS provides $ABTS^{\bullet+}$, which may be followed at 660 nm. In the absence of ABTS reactions were followed by monitoring the iron(III) porphyrin Soret band. With ABTS, the following reaction conditions with *t*-BuOOH are typical: reactions were carried out in aerobic solution with $[(2)Fe^{III}(H_2O)(X)]_i < [t\text{-BuOOH}] \ll [ABTS]_i$. The *t*-BuOOH was in 10–80-fold excess over $(2)Fe^{III}(H_2O)(X)$ catalyst, whose concentration ranged from 10^{-7} to 10^{-6} M. The concentration of ABTS was maintained at 2.0×10^{-2}–2.0×10^{-3} M. Formation

(4) (a) Kaaret, T. W.; Bruice, T. C. Unpublished results. (b) Sawyer, D. T.; Roberts, J. L., Jr. *Acc. Chem. Res.* **1988**, *21*, 469.

(5) (a) Bell, R. P. *The Proton in Chemistry*; Cornell University Press: Ithaca, NY, 1973. (b) Bruice, T. C.; Benkovic, S. J. *Bioorganic Mechanisms Volume 1*; W. A. Benjamin: New York, 1966; Chapter 1. (c) Jenks W. P. *Catalysis in Chemistry and Enzymology*; McGraw-Hill: New York, Chapter 1V, 1969.

(6) (a) Charton, M. *J. Org. Chem.* **1964**, *29*, 1222. (b) Fox, J. P.; Jencks, W. P. *J. Am. Chem. Soc.* **1974**, *96*, 1448. (c) Ballinger, P.; Long, F. A. *J. Am. Chem. Soc.* **1960**, *82*, 795.

(7) Panicucci, R.; Bruice, T. C. *J. Am. Chem. Soc.*, preceding paper in this issue.

(8) (a) Geibel, J.; Cannon, J.; Campbell, D.; Traylor, T. G. *J. Am. Chem. Soc.* **1978**, *100*, 3575. (b) Traylor, T. G.; White, D. K.; Campbell, D. H.; Berzinis, A. P. *J. Am. Chem. Soc.* **1981**, *103*, 4932. (c) Traylor, T. G.; Koga, N.; Deardurff, L. A. *J. Am. Chem. Soc.* **1985**, *107*, 6504.

Table I. Dependence of k_{obsd} on $[t\text{-BuOOH}]_i$ at Constant $[(2)Fe^{III}(H_2O)(X)] = 7.00 \times 10^{-7}$ M, [ABTS] = 9.8×10^{-3} M and pH 7.25

$[t\text{-BuOOH}]_i$, M	k_{obsd}, s^{-1}	$[t\text{-BuOOH}]_i$, M	k_{obsd}, s^{-1}
2.73×10^{-5}	6.84×10^{-4}	1.08×10^{-4}	6.37×10^{-4}
5.45×10^{-5}	6.55×10^{-4}	1.35×10^{-4}	6.21×10^{-4}
8.15×10^{-5}	6.45×10^{-4}		

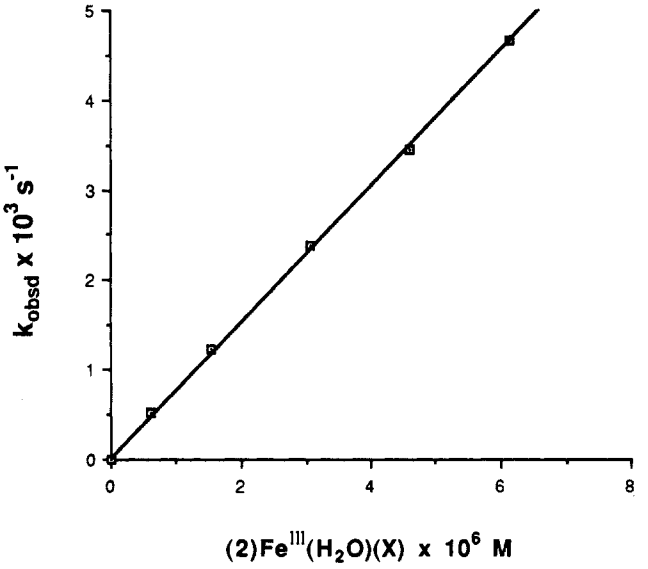

Figure 1. Observed first-order rate constants at pH 7.8 (0.05 M phosphate buffer 30 °C and $\mu = 0.2$) for the formation of ABTS$^{\bullet}$ as a function of $[(2)Fe^{III}(H_2O)(X)]$. The initial concentrations of t-BuOOH and ABTS were 5×10^{-5} and 7×10^{-3} M, respectively.

of ABTS$^{\bullet+}$ followed the first-order rate law, and the first-order rate constants (k_{obsd}) were linearly dependent on $[(2)Fe^{III}(H_2O)(X)]_i$ (a sampling of the data is shown in Figure 1 for the reaction at pH 7.8). Thus, the reaction is first-order in $(2)Fe^{III}(H_2O)(X)$. The yields of ABTS$^{\bullet+}$ were pH insensitive, ranging from 73% to 91%. Formation of ABTS$^{\bullet+}$ was not observed in the absence of either t-BuOOH or $(2)Fe^{III}(H_2O)(X)$.

Values of k_{obsd} were independent of the initial concentration of t-BuOOH ($[t\text{-BuOOH}]_i$) (Table I). The absorbance of ABTS$^{\bullet+}$ at completion of reaction was found to be directly proportional to $[t\text{-BuOOH}]_i$, and a plot of the absorbance vs $[t\text{-BuOOH}]_i$ had a slope of 1.97×10^4 M^{-1} cm^{-1}, corresponding to 82% yield of ABTS$^{\bullet+}$. Initial rates were obtained from plots of ΔA_{660} vs time (pH 7.25), and a plot of initial rates vs $[t\text{-BuOOH}]_i$ was linear with slope 9.63×10^{-4} s^{-1}. Taking into consideration the 82% yield of ABTS$^{\bullet+}$ and the fact that the rate of formation of ABTS$^{\bullet+}$ should be twice that of the disappearance of t-BuOOH, the mean value of the first-order rate constant of t-BuOOH consumption can be given as 5.9×10^{-4} s^{-1}, which is comparable to the average vlaue of the first-order appearance of ABTS$^{\bullet+}$ ($k_{obsd} = 6.5 \times 10^{-4}$ s^{-1}) at this pH. Thus, when the catalyst remains unsaturated in oxidant, the reaction follows the rate law of eq 4.

$$d(2[ABTS^{\bullet+}])/dt = -d[t\text{-BuOOH}]/dt = k_{1y}[(2)Fe^{III}(H_2O)(X)][t\text{-BuOOH}] \quad (4)$$

$$k_{obsd} = k_{1y}[(2)Fe^{III}(H_2O)(X)]$$

The effect of buffer concentration on the rate of reaction with t-BuOOH in the presence of ABTS has been examined with the following buffers: $ClCH_2CO_2H/ClCH_2CO_2^-$ (pH 2.05 and 2.90), $CH_3CO_2H/CH_3CO_2^-$ (pH 3.95, 4.70, 5.20, and 5.60), $H_2PO_4^-/HPO_4^{2-}$ (pH 6.20, 6.80, and 7.80), 2,4,6-trimethylpyridine/2,4,6-trimethylpyridine·H^+ (pH 7.22, 8.35), and HCO_3^-/CO_3^{2-} (pH 8.80, 9.05, 9.85, 10.50, and 10.80). Reactions were carried out at four buffer concentrations spanning a 10-fold concentration range. The (oxy acid)/(oxy anion) buffers exhibited no more than a very minor positive effect (within 10% augmentation) on k_{obsd}. With 2,4,6-trimethylpyridine·H^+/2,4,6-trimethylpyridine buffers no change was observed in k_{obsd} at each pH.

Table II. Product Analysis for the Reactions of $(2)Fe^{III}(H_2O)(X)$ with t-BuOOH/$(2)Fe^{III}(X) = 8.09 \times 10^{-6}$ M, t-BuOOH = 3.85×10^{-4} M, and ABTS = 9.24×10^{-3} M

	product yields[a] (%)	
pH	$(CH_3)_3COH$	$(CH_3)_2CO$
5.69	90	14
7.25	82	16
7.25[b]	81	16
7.25[c]	4	96
7.88	83	17
10.13	86	17
11.48	83	8
12.56	82	7
13.00	84	8

[a] Based on $[t\text{-BuOOH}]_i$. [b] Reaction carried out under anaerobic conditions. [c] No ABTS.

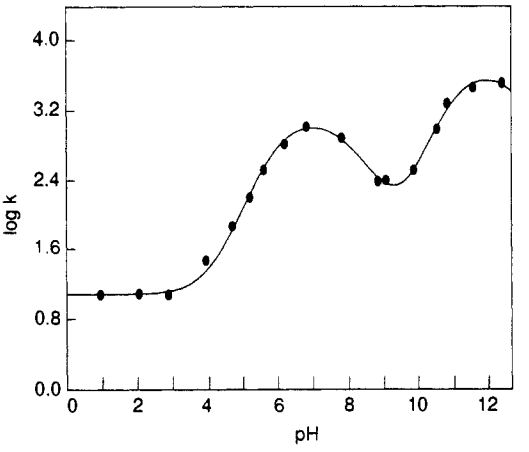

Figure 2. The pH dependence of the log of the nonbuffer-catalyzed rate constant (k_{1y}) for the reaction of $(2)Fe^{III}(H_2O)(X)$ with t-BuOOH in the presence of ABTS.

The pH dependence of the second-order rate constant, k_{1y}, for the reaction of $(2)Fe^{III}(H_2O)(X)$ with t-BuOOH was examined at pH values between pH 1.0 and 12.35. Between pH 2.0 and 10.8, the (oxy acid)/(oxy anion) buffers described previously were employed. Buffering by H_2O/HO^- (KOH) is sufficient to maintain a constant pH > 10.8 and H_3O^+/H_2O (hydrochloric acid) at pH < 2.0. Below pH 4, there was found to be a zero-order formation of ABTS$^{\bullet+}$ superimposed on the more rapid pseudo-first-order reaction. In this pH range, the experiments were carried out under an O_2 free N_2 atmosphere, to avoid the O_2-dependent zero-order appearance of ABTS$^{\bullet+}$. The slope of the plots of k_{obsd} vs $[(2)Fe^{III}(H_2O)(X)]_i$ provides k_{1y} (Figure 1). The yields of ABTS$^{\bullet+}$ (70–90% between pH 1.0 and 10.0 were obtained from ΔA_{660}. Above pH 10.0 the absorbance of ABTS$^{\bullet+}$ increases and then decreases with time due to oxidation of ABTS$^{\bullet+}$. At high pH, values of k_{obsd} for ABTS$^{\bullet+}$ formation were obtained by fitting the time course of A_{660} with a computer program for two consecutive first-order reactions.

A plot of log k_{1y} vs pH for reaction of $(2)Fe^{III}(H_2O)(X)$ with t-BuOOH in the presence of ABTS is shown in Figure 2. The points are experimental, and the line correlating the points was computer generated from a theoretical equation developed from Scheme I (Discussion section).

The products from the reaction of t-BuOOH with $(2)Fe^{III}(H_2O)(X)$ in the presence of ABTS were determined by GC by using calibration curves for quantitation (Table II). Reactions were run in sealed glass vials. Analysis of the spent reaction solutions was carried out on solutions with a ratio of catalyst/oxidant/ABTS = 1:48:1142. In the presence of ABTS, t-BuOH is obtained in 80–90% yield. The product distribution is independent of pH, buffer, and O_2. The combined yields of t-BuOH and $(CH_3)_2CO$ account for almost all the t-BuOOH. Methanol

Table III. Product Analysis for the Reaction of Cumyl Hydroperoxide (9.45×10^{-4} M) with (**2**)$Fe^{III}(H_2O)(X)$ (5.42×10^{-5} M) at $\mu = 0.20$ ($NaNO_3$)

pH	$[ABTS]_i$, M	$[PhCOCH_3]$, M	% yield
2.56	0	3.42×10^{-4}	35
2.56	7.16×10^{-3}	1.98×10^{-4}	21
7.25	0	7.24×10^{-4}	77
7.25	7.16×10^{-3}	2.67×10^{-4}	28
12.56	0	5.00×10^{-4}	53
12.56	7.16×10^{-3}	7.45×10^{-5}	8

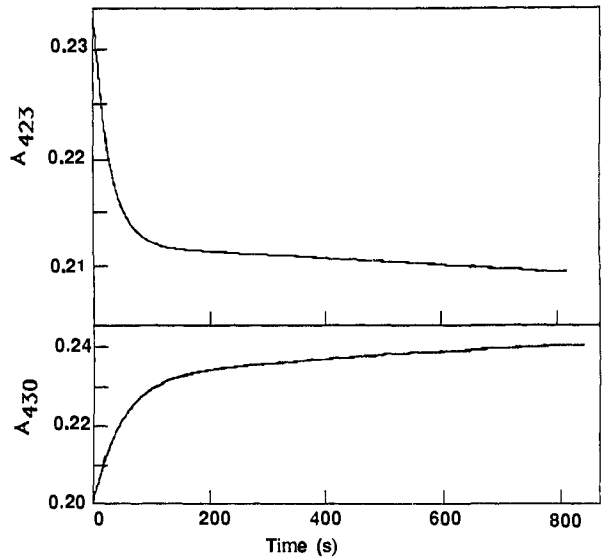

Figure 3. A plot of the changes in absorbance vs time for the reaction of $[t\text{-BuOOH}]_i$ (3.5×10^{-5} M) with [(**2**)$Fe^{III}(H_2O)(X)$] (5.0×10^{-6} M), 68 mM phosphate buffer, pH 7.25, $\mu = 0.20$ with $NaNO_3$) at 30 °C. Figure A corresponds to the changes in absorbance at 423 nm, and B corresponds to the changes in absorbance at 430 nm.

is the expected coproduct from the conversion of the four-carbon *t*-BuOOH to the three-carbon $(CH_3)_3CO$. Several runs carried out at high [*t*-BuOOH] (4.15×10^{-2} M) established CH_3OH as a product, since using *t*-BuOOH at 10^{-4} M, GC determination of methanol in aqueous solutions is unreliable.[2c]

At the same concentrations of (**2**)$Fe^{III}(H_2O)(X)$ and *t*-BuOOH as described above, with [ABTS] at 1.0×10^{-2} M, the reactions were investigated employing an oxygen electrode in a sealed reaction chamber at pH 7.25 and 10.13. No oxygen evolution was detected.

The Products from the Reaction of *t*-BuOOH with (2)$Fe^{III}(H_2O)(X)$, in the Absence of ABTS. At pH 7.25 with $[t\text{-BuOOH}]_i = 3.8 \times 10^{-4}$ M and (**2**)$Fe^{III}(H_2O)(X) = 8.1 \times 10^{-6}$ M, products are $(CH_3)_2CO$ (96%) and *t*-BuOH (4%). Assays for $(CH_3)_2CO$ at pH values 5.19, 8.10, 10.37, and 12.37 showed ~90% yields. $(t\text{-BuOO})_2$ could not be detected. In order to quantitate the yield of CH_3OH a concentration of *t*-BuOOH = 4.15×10^{-2} M was required ($[(2)Fe^{III}(H_2O)(X)]_i = 5.64 \times 10^{-5}$ M). At these concentrations of reactants there was detected $(CH_3)_2CO$ (94%) and CH_3OH (50%). GC–MS analysis of the nitrogen head space in the vials showed that neither CH_4 nor C_2H_6 was formed. When reactions were carried out in a sealed reaction chamber with an oxygen electrode at pH 7.25, by using the same concentrations of reagents as described above, no oxygen was detected.

Product analysis for the reaction of $Ph(CH_3)_2COOH$ (9.45×10^{-4} M) with (2)$Fe^{III}(H_2O)(X)$ (5.42×10^{-5} M) in the presence and absence of ABTS was carried out by HPLC at three pH values in sealed vials (Table III). Inspection of Table III shows that, in the presence or absence of ABTS, the maximum yield of acetophenone is obtained at pH 7.25. Neither PhOH nor $(CH_3)_2CO$ could be detected as products at any pH employed.

The Reaction of (2)$Fe^{III}(H_2O)(X)$ with *t*-BuOOH in the Absence of ABTS at pH 7.25 Gives Rise to an Observable Iron(IV)-Oxo Porphyrin Intermediate. With a 7-fold excess of *t*-BuOOH over (**2**)$Fe^{III}(H_2O)(X)$ (5.0×10^{-6} M), a biphasic dis-

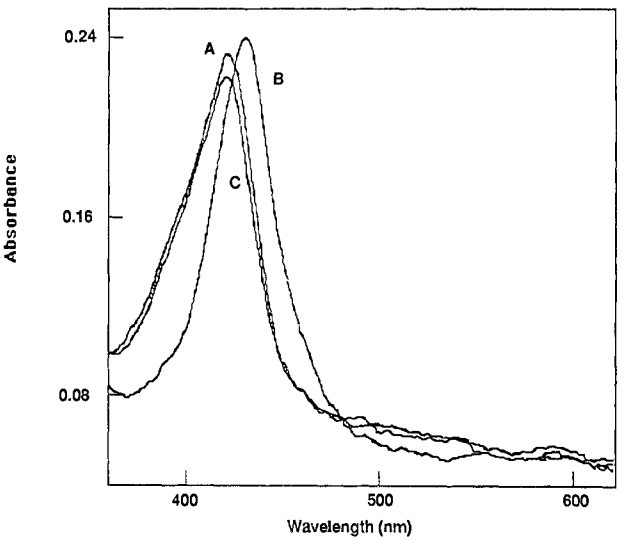

Figure 4. Spectra of a reaction mixture of (**2**)$Fe^{III}(H_2O)(X)$ (5.0×10^{-6} M) with $[t\text{-BuOOH}]_i$ (3.5×10^{-5} M) at pH 7.25 (68 mM phosphate buffer, $\mu = 0.20$ with $NaNO_3$, 30 °C). Spectrum A corresponds to that of (**2**)$Fe^{III}(H_2O)(X)$ before addition of *t*-BuOOH. B is a spectrum of iron(IV) species upon completion of reaction, and C is the final spectrum of the regenerated (**2**)$Fe^{III}(H_2O)(X)$.

appearance of the Soret band (423 nm) of (**2**)$Fe^{III}(H_2O)(X)$ is accompanied by the formation of an intermediate absorbing at 430 nm (Figure 3). The decrease in the Soret band (A_{423}) could be fitted to the appropriate equation for two sequential first-order processes. After all the *t*-BuOOH has been consumed, the iron(IV)-oxo porphyrin (A_{430}) decomposes over an ~80-h period to regenerate the original (**2**)$Fe^{III}(H_2O)(X)$ spectrum (>96%) (Figure 4). With sufficient [*t*-BuOOH] (3.5×10^{-5} M), the addition of ABTS (1.0×10^{-4} M), at some time after maximal appearance of absorbance at 430 nm, affords approximately 2.41 equiv of $ABTS^{\bullet+}$ based on $[(2)Fe^{III}(H_2O)(X)]_i$. Of these, 0.39 equiv of $ABTS^{\bullet+}$ are formed momentarily, and 2.02 equiv arise with a second-order rate constant comparable to that for reaction of *t*-BuOOH with (**2**)$Fe^{III}(H_2O)(X)$. These observations are explained as follows: at the time of maximal appearance of absorbance at 430 nm, 0.39 equiv of initial (**2**)$Fe^{III}(H_2O)(X)$ is present as an (**2**)$Fe^{IV}(O)(X)$ species which is instantly reduced by ABTS to provide $ABTS^{\bullet+}$ + (**2**)$Fe^{III}(H_2O)(X)$; the slow formation of remaining $ABTS^{\bullet+}$ arises from turnover of the (**2**)$Fe^{III}(H_2O)(X)$ catalyst on reacting with remaining *t*-BuOOH. During catalytic turnover in the presence of ABTS the (**2**)$Fe^{IV}(O)(X)$ species is reduced to (**2**)$Fe^{III}(H_2O)(X)$ immediately on its formation. From the value of A_{430} at the time of addition of ABTS, the spectral properties of the iron(IV) porphyrin can be determined as approximately λ_{max} 430 nm [ϵ_{max} (1.0 ± 0.1) $\times 10^5$ M^{-1} cm^{-1}].

Formation of an Iron(IV)-Oxo Species at Various pH Values between pH 2.0 and 12. Reaction of (**2**)$Fe^{III}(H_2O)(X)$ (5.0×10^{-6} M) with a 7-fold excess of *t*-BuOOH at pH 6.3, 10.37, and 11.68 also generates an intermediate with λ_{max} at 430 nm. The spectrum of the product and the dynamics for its formation are much the same as noted at pH 7.25 (Figure 5). Decomposition of the intermediate, after the consumption of *t*-BuOOH is complete, occurs over 100-h (pH 6.3), 50-h (pH 10.37), and 24-h (pH 11.68) periods to regenerate (**2**)$Fe^{III}(H_2O)(X)$ in >95%, 100%, and >97% yields, respectively. The species (**2**)$Fe^{IV}(O)(X)$ at pH 6.3 exhibits a λ_{max} at 430 nm. Knowing the yields of $ABTS^{\bullet+}$ formed by adding a 20-fold excess of ABTS after complete formation of iron(IV)-oxo intermediate allowed the determination of its concentration and calculation of an ϵ_{max} of (7.3 ± 0.3) $\times$ 10^4 M^{-1} cm^{-1} at 430 nm.

With a 7-fold excess of *t*-BuOOH over (**2**)$Fe^{III}(H_2O)(X)$ at pH 5.19 and 4.87, there occur biphasic decreases in absorbance at 404 nm ((**2**)$Fe^{III}(H_2O)_2$) and 423 nm ((**2**)$Fe^{III}(H_2O)(OH)$). The stable intermediate possesses the same λ_{max} as does the

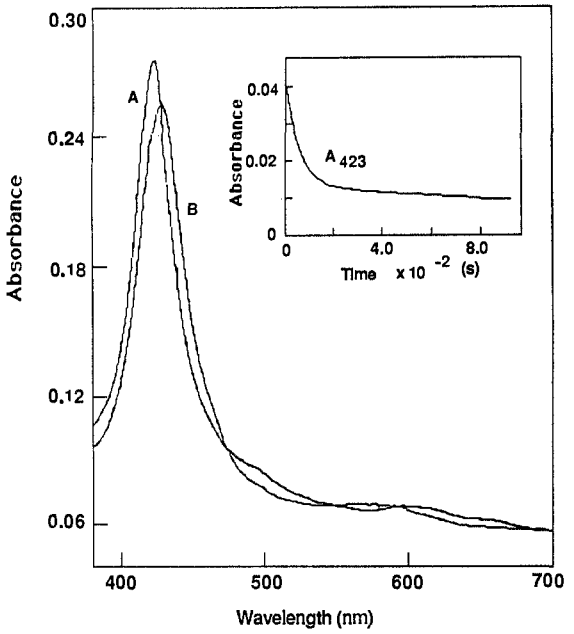

Figure 5. Spectra of a reaction mixture of (2)$Fe^{III}(H_2O)(X)$ (5.0×10^{-6} M) with $[t\text{-BuOOH}]_i$ (3.5×10^{-5} M) at pH 10.37. Spectrum A corresponds to that of (2)$Fe^{III}(H_2O)(X)$ before addition of *t*-BuOOH, and B is the spectrum of iron(IV) species upon completion of reaction. Inset: A plot of the change in absorbance at 423 nm vs time for the reaction of (2)$Fe^{III}(H_2O)(X)$ (5.0×10^{-6} M) with $[t\text{-BuOOH}]_i$ (3.5×10^{-5} M) at pH 10.37 (68 mM carbonate buffer, $\mu = 0.20$ with $NaNO_3$ at 30 °C).

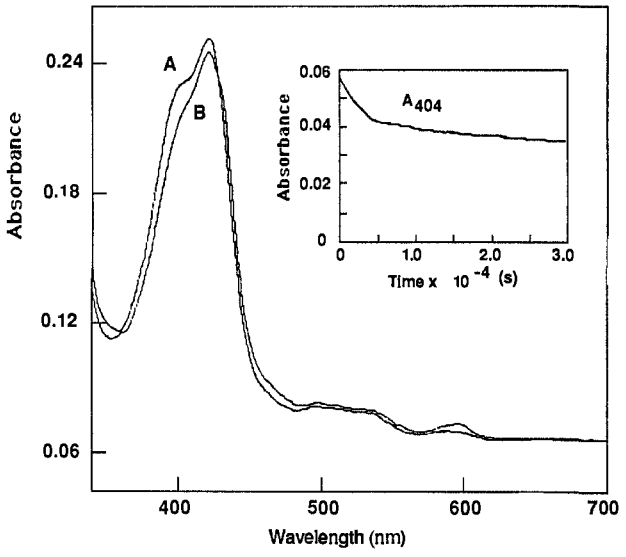

Figure 6. Spectra of a reaction mixture of (2)$Fe^{III}(H_2O)(X)$ (5.0×10^{-6} M) with $[t\text{-BuOOH}]_i$ (3.5×10^{-5} M) at pH 4.87. A is the spectrum of (2)$Fe^{III}(H_2O)(X)$ prior to addition of *t*-BuOOH, and B is the spectrum of iron(IV) species upon completion of reaction. Inset: A plot of the change in absorbance at 404 nm vs time for the reaction of (2)$Fe^{III}(H_2O)(X)$ (5.0×10^{-6} M) with $[t\text{-BuOOH}]_i$ (3.5×10^{-6} M) at pH 4.87 (68 mM acetate buffer, $\mu = 0.20$ with $NaNO_3$ at 30 °C).

iron(III) species at these pH values. Isosbestic points are seen at 429 and 360 nm [Figure 6 (pH 4.87)]. The iron(IV)-oxo intermediates decompose over ~70 h to regenerate the original Fe^{III} species (>95%). Again, addition of a 20-fold excess of ABTS (1.0×10^{-4} M), at some time after complete formation of the intermediate (Figure 6, inset), results in the latters reduction to (2)$Fe^{III}(H_2O)(X)$. The approximate spectral property of the species at pH 4.87 is λ_{max} 423 nm [ϵ_{max} (9.01 ± 0.05) $\times 10^4$ M^{-1} cm^{-1}].

Reaction of *t*-BuOOH with (2)$Fe^{III}(H_2O)(X)$ at a more acidic pH (3.73 and 2.56) results in a very small increase in the Soret bands at 423 and 404 nm followed by a continuous decrease in

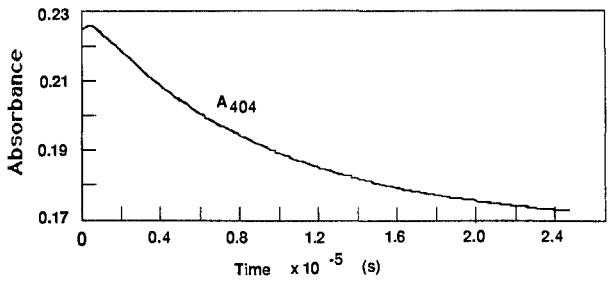

Figure 7. A plot of the change in absorbance at 404 nm vs time for the reaction of (2)$Fe^{III}(H_2O)(X)$ (5.0×10^{-6} M) with $[t\text{-BuOOH}]_i$ (3.5×10^{-6} M) at pH 2.56 (68 mM chloroacetic buffer, $\mu = 0.20$ with $NaNO_3$ at 30 °C).

absorbance (Figure 7) which continues for over 100 h. The loss in (2)$Fe^{III}(H_2O)(X)$, due to oxidative destruction, amounts to 13% at pH 3.73 and 28% at pH 2.56. On standing, the initial absorbance is not returned.

Above pH 12, addition of *t*-BuOOH results in a continuous decrease (5% loss based on $[(2)Fe^{III}(H_2O)(X)]_i$) in the Soret band (436 nm) until *t*-BuOOH is consumed. There is seen no intervening shift of the initial Soret band of the (2)$Fe^{III}(H_2O)(X)$ species, nor is there any return of the (2)$Fe^{III}(H_2O)(X)$ spectrum.

Formation of Iron(IV)-Oxo Porphyrin on Reaction of (2)-$Fe^{III}(H_2O)(X)$ (5.0×10^{-6} M) with *p*-$NO_2C_6H_4CO_3H$, *m*-$ClC_6H_4CO_3H$, $PhCH_2CO_3H$, $Ph_2(CN)COOH$, $Ph_2(CO_2CH_3)$-COOH, and $Ph(CH_3)_2COOH$ at pH 7.25 and 2.56 in the Absence of ABTS. In the presence of a 7-fold excess of each of the oxidants there is observed the formation of the same intermediate (λ_{max} 430 nm, at pH 7.25) seen with *t*-BuOOH. With the hydroperoxides (pH 7.25) $Ph_2(CN)COOH$, $Ph_2(CO_2CH_3)COOH$, and $Ph(CH_3)_2COOH$ the (2)$Fe^{IV}(O)(X)$ gives way to the original (2)$Fe^{III}(H_2O)(X)$ in ~21 h (>83%), 20 h (>98%), and 93 h (>97%), respectively. With the percarboxylic acid $PhCH_2CO_3H$, an ~90% loss in (2)$Fe^{IV}(O)(X)$ occurs over a 4-h period, without regeneration of (2)$Fe^{III}(H_2O)(X)$. For *m*-$ClC_6H_4CO_3H$, there is >50% loss after 5 h, and <40% of (2)$Fe^{III}(H_2O)(X)$ is regenerated. When using only a 1.5-fold excess of either *m*-$ClC_6H_4CO_3H$ or $PhCH_2CO_3H$, the (2)$Fe^{IV}(O)(X)$ decomposes with 90% regeneration of (2)$Fe^{III}(H_2O)(X)$ (Figure 8B). The appearance of A_{430} is shown in Figure 8A, where stopped-flow rapid-scan spectrophotometry was employed to follow the reaction with *m*-$ClC_6H_4CO_3H$. Inspection of Figure 8 shows that disappearance of iron(III) species (A_{423}) is accompanied by an increase in iron(IV)-oxo species (A_{430}) followed by a decrease in A_{430} and reappearance in A_{423}.

An pH 2.56, addition of *p*-$NO_2C_6H_4CO_3H$ is accompanied by an increase in absorbance with a small (3 nm) bathochromic shift in the Soret band (Figure 9A). This is then followed by a decrease in absorbance (Figure 9B) Formation of (2)$Fe^{IV}(O)(X)$ is associated with an isosbestic point at 569 nm.

The reaction of (2)$Fe^{III}(H_2O)(X)$ (5.0×10^{-6} M) with H_2O_2 (a 20-fold excess) in the absence of ABTS was followed at pH 7.25 by repetitive spectral scanning (Figure 10). No buildup of iron(IV)-oxo porphyrin could be detected. A continual decrease in the Soret absorbance occurs, and when H_2O_2 is consumed there is a 75% loss of (2)$Fe^{III}(H_2O)(X)$ ($k_{decomposition} = 5.85 \times 10^{-4}$ s^{-1}). With a 7-fold excess of H_2O_2 a 55% loss of (2)$Fe^{III}(H_2O)(X)$ is seen.

Influence of O_2 on the Formation of Iron(IV)-Oxo Porphyrin. In the absence of O_2 (pH 7.25), the reaction of (2)$Fe^{III}(H_2O)(X)$ (6.0×10^{-6} M) with *t*-BuOOH (3.03×10^{-5} M) or Ph-$(CH_3)_2COOH$ (3.02×10^{-5} M) results in a 10% decrease of the Soret maximum at 423 nm. Exposing the reaction solutions to flowing O_2 is accompanied by the appearance (A_{430}) of iron-(IV)-oxo porphyrin intermediates. Thus, the presence of O_2 is required for the formation of the iron(IV)-oxo porphyrin intermediate when using *t*-BuOOH or $Ph(CH_3)_2COOH$. In contrast, when the reactions of (2)$Fe^{III}(H_2O)(X)$ (5.0×10^{-6} M) with *m*-$ClC_6H_4CO_3H$ (1.5×10^{-5} M), $Ph_2(CN)COOH$ (1.48×10^{-5} M), and $Ph_2(CO_2CH_3)COOH$ (3.18×10^{-5} M) were carried out

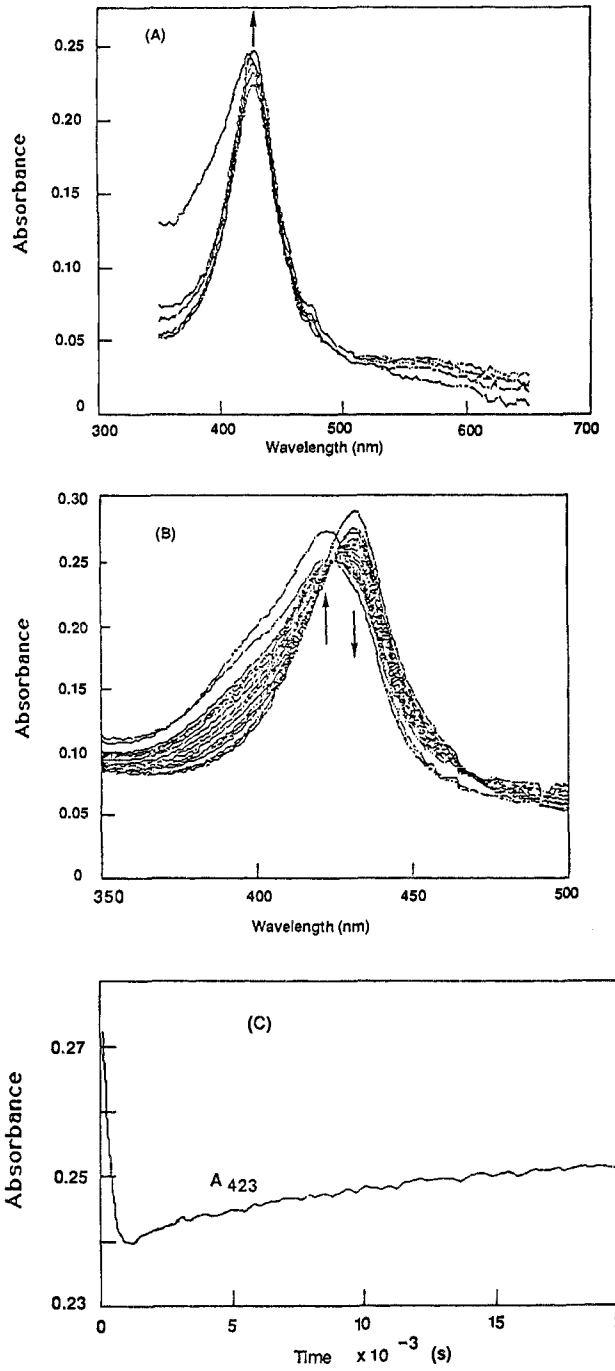

Figure 8. The reaction of (**2**)$Fe^{III}(H_2O)(X)$ with *m*-$ClC_6H_4CO_3H$ at pH 7.25 (68 mM phosphate buffer, μ = 0.20 with $NaNO_3$, 30 °C). Part A corresponds to the initial decrease in the absorbance at 423 nm and a simultaneous increase in absorbance at 430 nm. Reactions were followed by a rapid-scan stopped-flow apparatus. Part B corresponds to disappearance of the 430-nm species and a regeneration of the 423-nm species. Part C is a plot of the change in absorbance at 423 nm vs time for the reaction of (**2**)$Fe^{III}(H_2O)(X)$ (5.0×10^{-6} M) with [*m*-$ClC_6H_4CO_3H$]$_i$ (7.5×10^{-6} M) at pH 7.25.

under anaerobic conditions at pH 7.25 there is seen a decrease in A_{423} accompanied by an increase in A_{430}, followed by a regeneration of (**2**)$Fe^{III}(H_2O)(X)$ (A_{423}, >95%). Thus, oxygen is not required for the formation of the (**2**)$Fe^{IV}(O)(X)$ with these oxidants.

Carbon Monoxide Trapping of (2)$Fe^{II}(H_2O)(X)$. Under anaerobic conditions, addition of *t*-BuOOH (1.1×10^{-5} M) to a carbon monoxide saturated solution of (**2**)$Fe^{III}(H_2O)(X)$ (5.1×10^{-6} M) at pH 7.25 results in a shift of the Soret maximum from 423 to 427 nm with an increase in absorbance. With time the 427-nm absorbance decays, but, even after 92 h, the regeneration

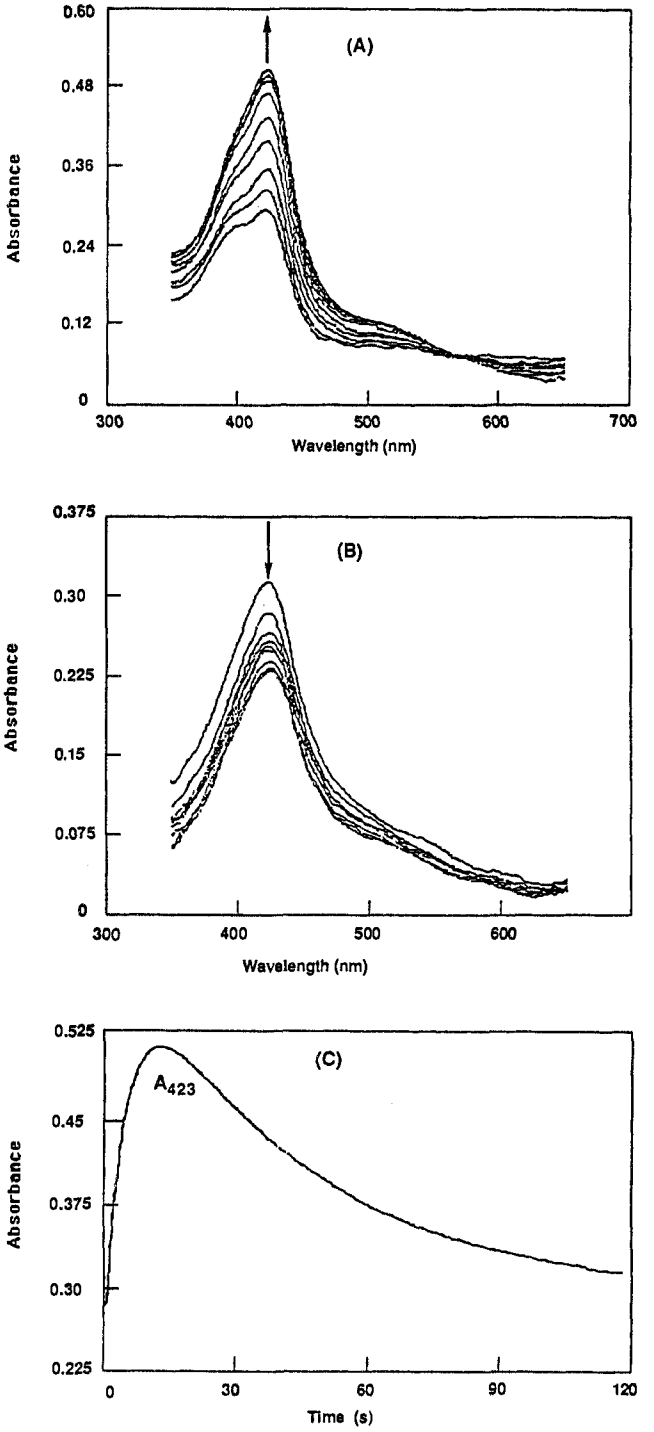

Figure 9. Rapid-scan stopped-flow reactions of (**2**)$Fe^{III}(H_2O)(X)$ with *p*-$NO_2C_6H_4CO_3H$ at pH 2.56 (μ = 0.20 with $NaNO_3$, 30 °C). Part A corresponds to the initial increase in the absorbance of Soret band, and part B corresponds to its subsequent decrease. Part C is a plot of the change in absorbance at 423 nm vs time.

of (**2**)$Fe^{III}(H_2O)(X)$ is not complete. Sodium dithionite (0.001 M) reduction of (**2**)$Fe^{III}(H_2O)(X)$ (under nitrogen, pH 7.25) results in the quantitative formation of (**2**)$Fe^{II}(H_2O)(X)$ (λ_{max} 439 nm, $\epsilon_{max} = 1.06 \times 10^5$ M^{-1} cm^{-1}), and saturation of the latter solution with CO generates (**2**)$Fe^{II}(CO)(X)$ (λ_{max} 427 nm, $\epsilon_{max} = 9.88 \times 10^4$ M^{-1} cm^{-1}) quantitatively.[8] Knowing the ϵ_{max} for (**2**)$Fe^{II}(CO)(X)$ and the observed 427-nm absorbance, it can be calculated that the yield of (**2**)$Fe^{II}(CO)(X)$ formed by the reaction of (**2**)$Fe^{III}(H_2O)(X)$ with *t*-BuOOH in the presence of CO is ca. 22%.

The reaction of *m*-$ClC_6H_4CO_3H$ (1.27×10^{-5} M) with (**2**)-$Fe^{III}(H_2O)(X)$ (5.0×10^{-6} M) at pH 7.25 in a CO saturated

Scheme I[a]

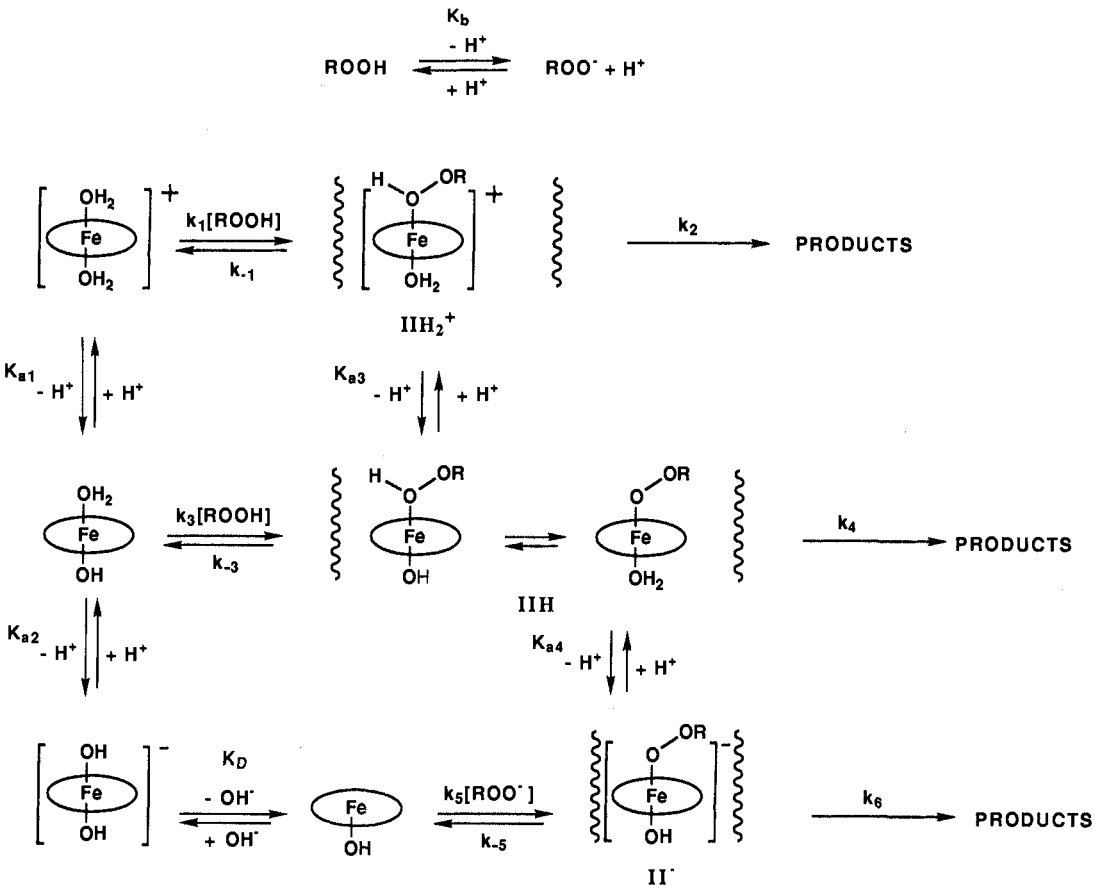

[a] All Fe are in +3 oxidation state.

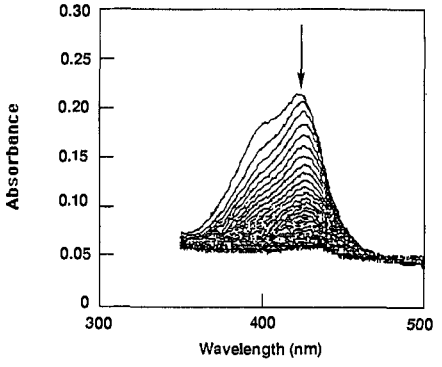

Figure 10. Repetitive scanning of a reaction mixture of (**2**)$Fe^{III}(H_2O)(X)$ (5.02×10^{-6} M) with $[H_2O_2]_i$ (1.04×10^{-4} M) at pH 6.3 (68 mM phosphate buffer, μ = 0.20 with $NaNO_3$, 30 °C).

buffered solution leads to the generation of the iron(IV)-oxo species (λ_{max} 430) followed by a regeneration of (**2**)$Fe^{III}(H_2O)(X)$ (>80% in 1 h, based on [(**2**)$Fe^{III}(H_2O)(X)$]. No (**2**)$Fe^{II}(H_2O)(CO)$ could be detected spectrophotometrically.

Discussion

Product and kinetic studies have been carried out for the reaction of [5,10,15,20-tetrakis(2,6-dichloro-3-sulfonatophenyl)-porphinato]iron(III) hydrate [(**2**)$Fe^{III}(X)_2$, X = H_2O or HO^-] with the YOOH compounds *t*-BuOOH, $Ph(CH_3)_2COOH$, $Ph_2(CO_2CH_3)COOH$, $Ph_2(CN)COOH$, $PhCH_2CO_3H$, *m*-$ClC_6H_4CO_3H$, and *p*-$NO_2C_6H_4CO_3H$ in water (pH 1–12.35, 30 °C with μ = 0.20 ($NaNO_3$)). Reactions are first-order in YOOH and (**2**)$Fe^{III}(H_2O)(X)$ at all pH values in the presence or absence of the easily oxidizable trap ABTS.

The pH dependence of the second-order rate constant for the reaction of *t*-BuOOH with (2)$Fe^{III}(X)_2$ is shown in Figure 2. The points of Figure 2 are experimental, and the line which fits the points has been generated from a kinetic equation (based on Scheme I) whose development is now discussed.

The proposed series of reactions is shown in Scheme I, where products arise via decomposition of IIH_2^+, IIH, and II^- (eq 5).

$$v = \frac{-d(t\text{-BuOOH})}{dt} = k_2[IIH_2^+] + k_4[IIH] + k_6[II^-] \quad (5)$$

The sum of the concentration of all intermediates is given by $[II_t] = [IIH_2^+] + [IIH] + [II^-]$. The concentration of each species is expressed as a mole fraction of $[II_t]$ in eqs 6, 7, and 8. Sub-

$$[II^-] = \frac{K_{a3}K_{a4}}{(K_{a3}K_{a4} + K_{a3}a_H + a_H^2)}[II_t] \quad (6)$$

$$[IIH] = \frac{a_H K_{a3}}{(K_{a3}K_{a4} + K_{a3}a_H + a_H^2)}[II_t] \quad (7)$$

$$[IIH_2^+] = \frac{a_H^2}{(K_{a3}K_{a4} + K_{a3}a_H + a_H^2)}[II_t] \quad (8)$$

stituting the equalities of eqs 6, 7, and 8 into eq 5 provides eq 9, and steady-state assumption in $[II_t]$ provides eq 10. Substituting

$$v = \frac{k_2a_H^2 + k_4K_{a3}a_H + k_6K_{a3}K_{a4}}{(K_{a3}K_{a4} + K_{a3}a_H + a_H^2)}[II_t] \quad (9)$$

the value of $[II_t]$ (eq 10) into eq 9 and rearranging provides the full expression for the pH sensitive second-order rate constant k_{ly} (eq 11), where $[Fe_t]$ represents the concentration of all iron porphyrin species and $[ROOH_t] = [t\text{-BuOOH}] + [t\text{-BuOO}^-]$

$$[II_t] = \frac{(k_1a_H^3 + k_3K_{a1}a_H^2 + k_5(K_D/K_W)K_{a1}K_{a2}K_ba_H)(K_{a3}K_{a4} + a_HK_{a3} + a_H^2)[Fe_t][ROOH_t]}{((k_2 + k_{-1})a_H^2 + (k_4 + k_{-3})a_HK_{a3} + (k_6 + k_{-5})K_{a3}K_{a4})(a_H^2 + K_{a1}a_H + K_{a1}K_{a2})(K_b + a_H)} \quad (10)$$

Scheme II[a]

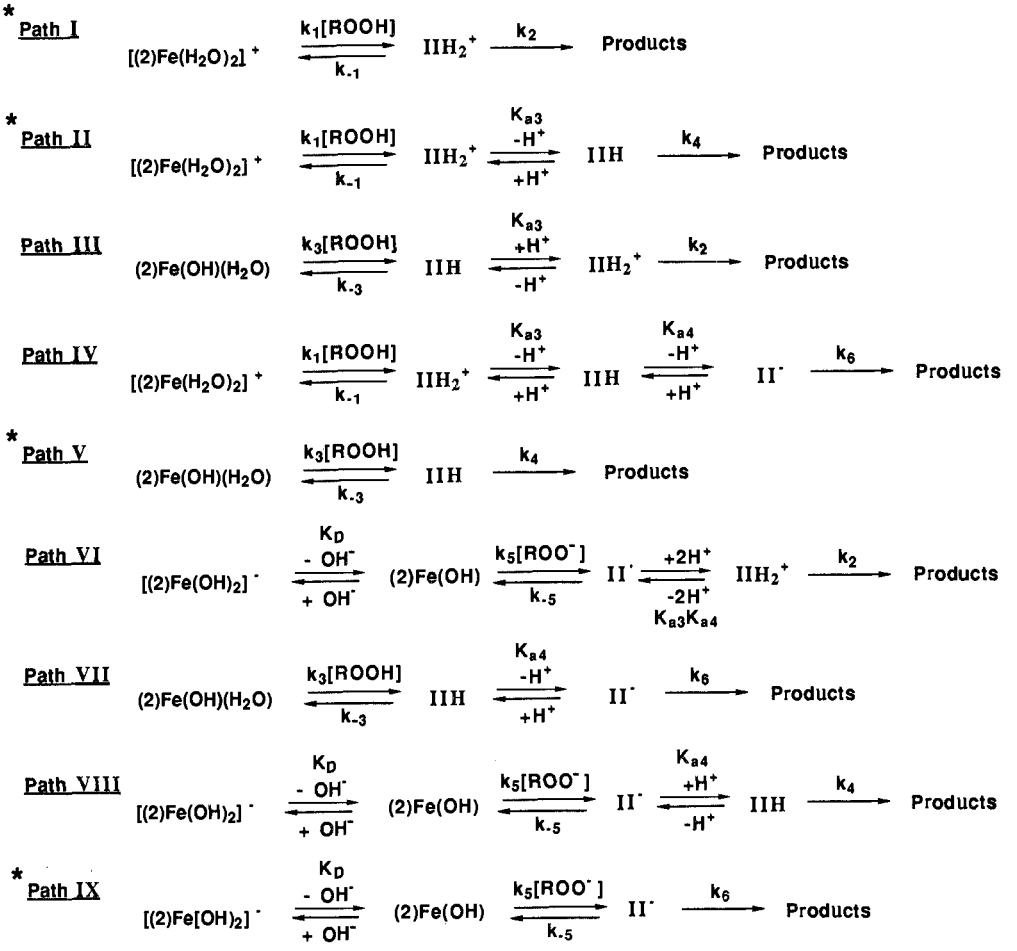

[a] All Fe are in +3 oxidation state.

Computer fitting of the experimental points by use of eq 11 provides a set of constants. Knowledge of their relative values

$$k_{1y} = \frac{k_2k_1a_H}{(k_2 + k_{-1})} \frac{\left\{\frac{a_H^2 + k_4K_{a3}a_H + k_6K_{a3}K_{a4}}{k_2}\right\}\left\{\frac{a_H^2 + k_3K_{a1}a_H + k_5K_DK_{a1}K_{a2}K_b}{k_1K_w}\right\}}{\left\{\frac{a_H^2 + (k_4 + k_{-3})a_HK_{a3} + (k_6 + k_{-5})K_{a3}K_{a4}}{(k_2 + k_{-1})}\right\}(a_H^2 + K_{a1}a_H + K_{a1}K_{a2})(K_b + a_H)}$$

$$= \frac{A(a_H^5 + Ba_H^4 + Ca_H^3 + Da_H^2 + Ea_H)}{\left\{\frac{a_H^2 + (k_4 + k_{-3})a_HK_{a3} + (k_6 + k_{-5})K_{a3}K_{a4}}{(k_2 + k_{-1})}\right\}(a_H^2 + K_{a1}a_H + K_{a1}K_{a2})(K_b + a_H)} \quad (11)$$

where

$$A = \frac{k_2k_1}{(k_2 + k_{-1})} \qquad B = \frac{k_4K_{a3}}{k_2} + \frac{k_3K_{a1}}{k_1} \qquad C = \frac{k_4k_3K_{a3}K_{a1}}{k_2k_1} + \frac{k_5K_DK_{a1}K_{a2}K_b}{k_1K_w} + \frac{k_6K_{a3}K_{a4}}{k_2}$$

$$D = \frac{k_4k_5K_DK_{a1}K_{a2}K_{a3}K_b}{k_2k_1K_w} + \frac{k_3k_6K_{a1}K_{a3}K_{a4}}{k_2k_1} \qquad E = \frac{k_6k_5K_DK_{a1}K_{a2}K_{a3}K_{a4}K_b}{k_2k_1K_w}$$

allows simplification of eq 11 in the different pH regions. At low pH (<3) k_{1y} is independent of pH and $a_H \gg K_{a1}$, K_{a2}, K_{a3}, K_{a4}, K_b such that eq 11 reduces to eq 12. Thus, in the plateau region at low pH the reaction is given by path I of Scheme II.

$$k_{1y} = A = \frac{k_2k_1}{(k_2 + k_{-1})} \quad [12]$$

Between pH 3.5 and 9 the dependence of log k_{1y} on pH describes a "bell-shaped" curve. Here, $K_b < a_H > K_{a2}$ so that eq 11 reduces to eq 13a. The terms $(k_4K_{a3}/k_2)Ya_H^2$ and $(k_3K_{a1}/k_1)Ya_H^2$ pertain to paths II and III (Scheme II), respectively. Either of the two terms would generate a "bell-shaped" pH profile between pH 3.5 and 8.5. If only the first pathway (path II) were to be operative, the rate increase in the ascending portion of the bell would result from the increased degree of ionization of IIH_2^+ to IIH with an

$$k_{1y} = BYa_H^2 + CYa_H \quad [13a]$$

where

$$Y = \frac{k_2k_1}{(k_2 + k_{-1})\left\{\frac{a_H^2 + (k_4 + k_{-3})a_HK_{a3} + (k_6 + k_{-5})K_{a3}K_{a4}}{(k_2 + k_{-1})}\right\}(a_H + K_{a1})}$$

increase in the pH, until the depletion of (2)$Fe^{III}(H_2O)(X)$ due to its ionization to (2)$Fe^{III}(HO)(X)$ would cause ligation of *t*-BuOOH to iron(III) porphyrin to become rate-limiting. This results in the drop in rate seen in the descending part of the "bell". Conversely the second and kinetically equivalent pathway (path III) would predict an increase in rate accompanying the ionization of (2)$Fe^{III}(H_2O)(X)$, and the decreased protonation of IIH at higher pH values would make its partitioning to products (via IIH_2^+) more unfavorable, leading to the drop in rate which characterizes the descending part of the "bell".

Similarly, each of the three terms in CYa_H would generate a "bell-shaped" profile when the pH is between 7 and 10. Thus in the pH region from 3.5 to 9.5 the change in log k_{1y} with pH results from two overlapping "bells". The terms $(k_6/k_2)K_{a3}K_{a4}Ya_H$, $(k_4k_3/k_2k_1)K_{a1}K_{a3}Ya_H$, and $(k_5/k_1)(K_D/K_W)K_{a1}K_{a2}K_b$ relate to paths IV, V, and VI of Scheme II, respectively. The reaction intermediates of Scheme I are identical with those proposed in the previous paper[7] for the reaction of hydrogen peroxide with (2)$Fe^{III}(X)_2$. The difference in the shapes of the log k_{1y} vs pH profiles for the reactions of *tert*-butyl hydroperoxide and hydrogen peroxide with (2)$Fe^{III}(H_2O)(X)$ is due to preequilibrium ligation of hydrogen peroxide and steady-state formation of ligated *tert*-butyl hydroperoxide, respectively. Because of the relative simplicity of the log k_{1y} vs pH profile for the reaction with hydrogen peroxide it is possible to identify the species whose breakdown

represents the commitment steps. These are (2)$Fe^{III}(H_2O)(H_2O_2)$ (at low pH), (2)$Fe^{III}(H_2O)(HO_2^-)$ (medium pH), and (2)$Fe^{III}(HO^-)(HO_2^-)$ (at high pH). With the reasonable assumption that like species are involved in the commitment steps for the reaction with *tert*-butyl hydroperoxide [low ((2)$Fe^{III}(H_2O)(t\text{-}BuO_2H)$), medium ((2)$Fe^{III}(H_2O)(t\text{-}BuO_2^-)$), and high pH ((2)$Fe^{III}(HO^-)(t\text{-}BuO_2^-)$] a choice between the sets of kinetically equivalent reaction paths, describing intermediate pH region of the pH vs los k_{1y} profile, can be made. Thus, II and V are chosen over III, IV, and VI providing eq 13b, which describes the dependence of k_{1y} between pH 3.5 and 9.5.

$$k_{1y} = \frac{\frac{k_2k_1}{(k_2 + k_{-1})}\left\{\frac{k_4K_{a3}a_H^2}{k_2} + \frac{k_4k_3K_{a3}K_{a1}a_H}{k_2k_1}\right\}}{\left\{a_H^2 + \frac{(k_4 + k_{-3})a_HK_{a3}}{(k_2 + k_{-1})} + \frac{(k_6 + k_{-5})K_{a3}K_{a4}}{(k_2 + k_{-1})}\right\}(a_H + K_{a1})} \quad [13b]$$

Between pH 9 and 10 the pH dependence of k_{1y} may also include a contribution from the terms DYa_H (eq 14). The two component terms of eq 14 represent the contributions of paths VIII and VII

$$DYa_H = \left\{\frac{k_4k_5K_DK_{a1}K_{a2}K_{a3}K_b}{k_2k_1K_w} + \frac{k_3k_6K_{a1}K_{a3}K_{a4}}{k_2k_1}\right\}Ya_H \quad [14]$$

of Scheme II, respectively. However, fitting of eq 11 to the experimental data shows that the contribution of the DYa_H term to log k_{1y} is less than 30%, and exclusion of a DYa_H term provides as good a fit as with it. Therefore, a DYa_H term was not included in eq 16.

When pH > 10, eq 11 simplifies to eq 15. Here, the kinetic pathway is IX of Scheme II. The ascending part of the second "bell" results from a rate increase on increasing ionization of

$$k_{1y} = \frac{A\,Ea_H}{\frac{(k_6 + k_{-5})K_{a3}K_{a4}K_{a1}(a_H + K_{a2})(K_b + a_H)}{(k_2 + k_{-1})}}$$

$$= \frac{k_6k_5}{(k_6 + k_{-5})}\frac{(K_D/K_w)K_{a1}K_{a2}K_ba_H}{(a_H + K_{a2})(K_b + a_H)} \quad [15]$$

[(2)Fe(OH)(H_2O) ⇌ (2)$Fe(OH)_2$ + H^+] and [ROOH ⇌ ROO^- + H^+], with pH. With a further increase in pH, however, the high concentrations of OH^- present disfavor in the ligation of ROO^- and result in the decrease in rate disfavor which characterizes the descending arm of the "bell".

Summation of the terms contributing to k_{1y} at each pH region provides eq 16 which describes the dependence of k_{1y} on pH over the entire pH range using paths I, II, V, and IX. The best values of kinetic constants (Table IV) were obtained by computer fitting of the experimental points of Figure 2, by the line generated from eq 16. The value of the thermodynamic constant K_{a1} (Scheme I) has been determined by us,[7] and the value of K_b (K_b = [*t*-$BuOO^-$][H^+]/[*t*-BuOOH] = 1.6×10^{-13}) is reported in the literature.[9] Since, aside from K_{a2}, the individual rate and equilibrium constants of Scheme I appear in collections of terms, their independent values cannot be determined without further assumptions.

$$k_{1y} = \frac{k_2k_1}{(k_2 + k_{-1})} + \frac{\frac{k_2k_1}{(k_2 + k_{-1})}\left\{\frac{k_4K_{a3}a_H^2}{k_2} + \frac{k_4k_3K_{a3}K_{a1}a_H}{k_2k_1}\right\}}{\left\{a_H^2 + \frac{(k_4 + k_{-3})a_HK_{a3}}{(k_2 + k_{-1})} + \frac{(k_6 + k_{-5})K_{a3}K_{a4}}{(k_2 + k_{-1})}\right\}(a_H + K_{a1})} + \frac{\left\{\frac{k_6k_5K_DK_{a2}K_b}{(k_6 + k_{-5})K_w}\right\}a_H}{(a_H + K_{a2})(K_b + a_H)} \quad [16]$$

General-Base or General-Acid Catalysis. Previous investigations, in water, have involved studies of the reaction of hydrogen peroxide species with (2)$Fe^{III}(H_2O)(X)$[7] and the complexes of

Scheme III

(2)$Fe^{III}(H_2O)(X)$ + t-BuOOH ⟶ [(2)$Fe^{III}(X)$(t-BuOOH)] (I)

[(2)$Fe^{III}(X)$(t-BuOOH)] ⟶ (2)$Fe^{IV}(O)(X)$ + t-BuO· + H^+ (II)

(2)$Fe^{IV}(O)(X)$ + ABTS + $2H^+$ ⟶ (2)$Fe^{III}(H_2O)(X)$ + $ABTS^{\cdot+}$ (III)

t-BuO· + ABTS + H^+ ⟶ t-BuOH + $ABTS^{\cdot+}$ (IV)

t-BuO· ⟶ $(CH_3)_2C{=}O$ + CH_3· (V)

CH_3· + (2)$Fe^{IV}(O)(X)$ + H^+ ⟶ CH_3OH + (2)$Fe^{III}(H_2O)(X)$ (VI)

5,10,15,20-tetrakis(2,6-dimethyl-3-sulfonatophenyl)porphinatoiron(III) hydrate, (1)$Fe^{III}(H_2O)(X)$,[10] and (1)$Mn^{III}(H_2O)(X)$[11] as well as the reaction of *t*-BuOOH and $Ph(CH_3)_2COOH$ with (1)$Fe^{III}(H_2O)(X)$.[2a-c] It was shown that the reaction of *t*-BuOOH and $Ph(CH_3)_2COOH$ with (1)$Fe^{III}(H_2O)(X)$ is not catalyzed by oxy anion bases nor their conjugate acids. In this study we show that the pH-dependent second-order rate constants (k_{1y}) for reaction of *t*-BuOOH with (2)$Fe^{III}(X)_2$ are insensitive to the concentrations of buffer oxy anion bases and their conjugate acids over the pH range 2–10.8. Oxy anion bases and their conjugate acids do not catalyze the reaction of (1)$Fe^{III}(H_2O)(X)$[10] or (2)$Fe^{III}(H_2O)(X)$[7] with hydrogen peroxide. We have shown that substituted 2,6-dimethylpyridine·H^+/2,6-dimethylpyridine nitrogen base buffers exhibited no general (base or acid) catalysis in the reaction of *t*-BuOOH with (1)$Fe^{III}(H_2O)(X)$ or in the reaction of hydrogen peroxide with (1)$Mn^{III}(H_2O)(X)$.[11] The present study establishes that catalysis by substituted 2,6-dimethylpyridine·H^+/2,6-dimethylpyridine nitrogen base buffers is not seen in the reaction of *t*-BuOOH with (2)$Fe^{III}(X)_2$.

Of all the reactions of metal(III) porphyrins with hydroperoxides that we have investigated to date, a case for general catalysis is only seen with substituted 2,6-dimethylpyridine buffers in the reaction of hydrogen peroxide with (1)$Fe^{III}(H_2O)(X)$[10] and (2)$Fe^{III}(H_2O)(X)$[7] (discussed in the previous paper in this journal).

Products formed under trapping condition with ABTS at <pH 10 are $ABTS^{\cdot+}$ (~80%), *t*-BuOH (~80%), and $(CH_3)_2CO$ (15%), while at pH 11 they are $ABTS^{\cdot+}$ (<30%), *t*-BuOH (~80%), and $(CH_3)_2CO$ (<10%). The low yield of $ABTS^{\cdot+}$ at high pH is due to the rapid oxidation of $ABTS^{\cdot+}$ to the dication ($ABTS^{2+}$).[10] The products and their yields are independent of the presence or absence of O_2.

The products of *t*-BuOOH decomposition arise from the fragmentation of $(CH_3)_3CO^{\cdot}$ as shown in experiments with $Ph(CH_3)_2COOH$. From $Ph(CH_3)_2COOH$, formation of $Ph(CH_3)_2CO^+$ in water would yield phenol and acetone (eq 17). Formation of $Ph(CH_3)_2CO^{\cdot}$ would be followed by radical fragmentation to provide acetophenone and $CH_3^{\cdot}$ (eq 18).[13] In-

$$Ph(CH_3)_2CO^+ \rightarrow (CH_3)_2C^+OPh \xrightarrow{HO^-} (CH_3)_2C(OH)OPh \rightarrow (CH_3)_2C{=}O + PhOH \quad (17)$$

$$Ph(CH_3)_2CO^{\cdot} \rightarrow CH_3COPh + CH_3^{\cdot} \quad (18)$$

$$(2)Fe^{IV}(O)(X) + CH_3^{\cdot} \xrightarrow{H_2O} (2)Fe^{III}(H_2O)(X) + CH_3OH$$

spection of Table III shows that acetophenone is produced in the reaction of $Ph(CH_3)_2COOH$ with (2)$Fe^{III}(X)_2$ between pH 2 and 12.56. Neither PhOH nor $(CH_3)_2CO$ could be detected. Acetophenone is the product of fragmentation of $Ph(CH_3)_2CO^{\cdot}$. Alkoxyl radicals (*t*-BuO· and $Ph(CH_3)_2CO^{\cdot}$) are direct products of the homolytic scission of alkyl hydroperoxide O–O bonds (Scheme III). Reaction of *t*-BuO· with ABTS provides *t*-BuOH and $ABTS^{\cdot+}$ (>80%, Table II), while untrapped *t*-BuO· undergoes

(9) Everett, A. J.; Minkoff, G. J. *Trans. Faraday Soc.* **1953**, *49*, 410.

(10) Zipplies, M. F.; Lee, W. A.; Bruice, T. C. *J. Am. Chem. Soc.* **1986**, *108*, 4433.

(11) Balasubramanian, P. N.; Schmidt, E. S.; Bruice, T. C. *J. Am. Chem. Soc.* **1987**, *109*, 7865.

(12) Bruice, T. C.; Noar, J. B.; Ball, S. S.; Venkataram, *J. Am. Chem. Soc.* **1983**, *105*, 2462.

(13) Meehan, E. J.; Kolthoff, I. M.; Auerbach, C.; Minato, H. *J. Am. Chem. Soc.* **1961**, *83*, 2232.

Table IV. Values of Rate and Equilibrium Constants Used in the Fitting of the Line Defined by Eq 16 to the pH Dependence of the Apparent Second-Order Rate Constants (k_{ly}) for the Reaction of *t*-BuOOH with (**2**)$Fe^{III}(X)(H_2O)$

kinetic terms	values of determined constants	kinetic terms	values of determined constants
$k_2k_1/(k_2 + k_{-1})$	12.4 M^{-1} s^{-1}	$[(k_4 + k_{-3})/(k_2 + k_{-1})]K_{a3}$	1.0×10^{-6} M
		$[(k_6 + k_{-5})/(k_4 + k_{-3})]K_{a4}$	4.4×10^{-10} M
$(k_4/k_2)K_{a3}$	9.6×10^{-5} M	$[k_5k_6/(k_6 + k_{-5})]K_D$	2.68×10^2 s^{-1}
k_3/k_1	0.165	K_{a2}	9.6×10^{-12} M
K_{a1}	1.4×10^{-8} M	K_b	1.6×10^{-13} M

fragmentation to acetone (<15%) and $CH_3^{\bullet}$.[14] The (**2**)$Fe^{IV}(O)(X)$ species formed on homolytic reaction of *t*-BuOOH with (**2**)-$Fe^{III}(H_2O)(X)$ would react with either ABTS or $CH_3^{\bullet}$ to regenerate (**2**)$Fe^{III}(H_2O)(X)$ with formation of $ABTS^{\bullet+}$ or to yield CH_3OH, respectively.[2c] Processes which occur in the absence of ABTS will be considered (vide infra). The fragmentation of *t*-BuO$^{\bullet}$ in water and the bimolecular reaction of ABTS with *t*-BuO$^{\bullet}$ have been previously investigated.[14a] In this study, as in the study with (**1**)$Fe^{III}(H_2O)(X)$,[2c] neither $(t\text{-BuO})_2$ nor O_2 was detected in the presence of ABTS. Approximately 15% of $(CH_3)_2CO$ and 85% of *t*-BuOH are formed with ca. 80% of $ABTS^{\bullet+}$ (Table II). As an explicit interpretation, $(CH_3)_2CO$ is from fragmentation of *t*-BuO$^{\bullet}$ within a solvent cage (eq 19), and *t*-BuOH is from the reaction of free *t*-BuO$^{\bullet}$ with ABTS (eq 20). That the reaction of eq 19 does occur in a solvent cage has been shown in this and a previous study with 5,10,15,20-tetrakis(2,6-dimethyl-3-sulfonatophenyl)porphinatoiron(III) hydrate [(**1**)-$Fe^{III}(H_2O)(X)$].[2c] With (**1**)$Fe^{III}(H_2O)(X)$, an increase in the

$$[(\mathbf{2})Fe^{IV}(O)(X)\ {}^{\bullet}OC(CH_3)_3] \xrightarrow{20\%} (\mathbf{2})Fe^{III}(H_2O)(X) + (CH_3)_2CO + CH_3OH \quad (19)$$

$$(\mathbf{2})Fe^{IV}(O)(X) + ABTS + H^+ \rightarrow (\mathbf{2})Fe^{III}(H_2O)(X) + ABTS^{\bullet+} \quad (20a)$$

$$ABTS + {}^{\bullet}OC(CH_3)_3 + H_2O \rightarrow ABTS^{\bullet+} + (CH_3)_3COH + HO^- \quad (20b)$$

ABTS concentration provides increasing yields of $(CH_3)_3COH$, but at higher concentrations of ABTS an 85% yield of $(CH_3)_3$-COH (and 15% yield of $(CH_3)_2CO$) is asymptotically approached. In this study the limiting yields are 80% $(CH_3)_3COH$, eq 20, and 20% $(CH_3)_2CO$, eq 19.

Products Formed in the Absence of ABTS. In the absence of ABTS, the products of decomposition of *t*-BuOOH are $(CH_3)_2$-C=O, CH_3OH, and *t*-BuOH. A >90% yield of $(CH_3)_2C$=O is formed at pH values 5.19, 7.25, 8.10, 10.37, and 12.7. Neither CH_4, C_2H_6, O_2, or $(t\text{-BuO})_2$ could be detected as products. The reaction of (**2**)$Fe^{III}(H_2O)(X)$ with $Ph(CH_3)_2COOH$ at pH 7.25 provides $Ph(CH_3)C$=O in ~70% yield. No PhOH nor $(C-H_3)_2C$=O are formed. This, again, establishes that $Ph-(CH_3)_2COOH$ yields $Ph(CH_3)_2CO^{\bullet}$, in accord with a homolytic cleavage of the O–O bond of $Ph(CH_3)_2COOH$. The same observations and conclusions pertain to the reaction of $Ph-(CH_3)_2COOH$ and *t*-BuOOH with (**1**)$Fe^{III}(H_2O)(X)$.[2d]

The reaction of (**2**)$Fe^{III}(H_2O)(X)$ with *t*-BuOOH, particularly between pH 3 and 9, is now discussed in terms of Scheme IV. Additional support for the reactions of Scheme IV may be found in a previous study involving (**1**)$Fe^{III}(H_2O)(X)$.[2d] From this and the previous investigations it is appreciated that the reaction of (**1**)$Fe^{III}(H_2O)(X)$ and (**2**)$Fe^{III}(H_2O)(X)$ with alkyl hydroperoxides proceeds via initial ligation of the hydroperoxide (reaction A of Scheme IV).[2c] In reactions with *t*-BuOOH, a certain percentage of oxidizing intermediates are not trappable by ABTS (for (**1**)-$Fe^{III}(H_2O)(X)$ 15% and for (**2**)$Fe^{III}(H_2O)(X)$ 20%). From the

Scheme IV[a]

Association

(A) (**2**)$Fe^{III}(H_2O)(X) + (CH_3)_3COOH \rightarrow$ (**2**)$Fe^{III}(X)((CH_3)_3COOH)$

Caged Reactions

(B) (**2**)$Fe^{III}(X)((CH_3)_3COOH) \rightarrow \{$(**2**)$Fe^{IV}(O)(X)$, ${}^{\bullet}OC(CH_3)_3\}$

(C) $\{$(**2**)$Fe^{IV}(O)(X)$, ${}^{\bullet}OC(CH_3)_3\} \rightarrow \{$(**2**)$Fe^{IV}(O)(X)$, $CH_3^{\bullet}$, $O{=}C(CH_3)_2\}$

(D) $\{$(**2**)$Fe^{IV}(O)(X)$, $CH_3^{\bullet}$, $O{=}C(CH_3)_2\} \rightarrow$ (**2**)$Fe^{III}(H_2O)(X) + CH_3OH + (CH_3)_2CO$

Non - Caged reactions

(E) (**2**)$Fe^{III}(X)((CH_3)_3COOH) \rightarrow$ (**2**)$Fe^{IV}(O)(X) + (CH_3)_3C-O^{\bullet}$

(F) $(CH_3)_3C-O^{\bullet} \rightarrow (CH_3)_2C{=}O + CH_3^{\bullet}$

(G) (**2**)$Fe^{IV}(O)(X) + CH_3^{\bullet} \rightarrow$ (**2**)$Fe^{III}(H_2O)(X) + CH_3OH$

Following reactions

(H) (**2**)$Fe^{III}(H_2O)(X) + CH_3^{\bullet} \rightarrow$ (**2**)$Fe^{II}(X)(H_2O) + CH_3OH$

(I) $2 \times$ (**2**)$Fe^{II}(H_2O)(X) + O_2 \rightarrow$ (**2**)$Fe^{III}(X){-}O{-}O{-}Fe^{III}(X)$(**2**)

(J) (**2**)$Fe^{III}(X){-}O{-}O{-}Fe^{III}(X)$(**2**) $\rightarrow 2$ (**2**)$Fe^{IV}(O)(X)$

(K) (**2**)$Fe^{II}(H_2O)(X)$ + (**2**)$Fe^{IV}(O)(X) \rightarrow 2$ (**2**)$Fe^{III}(H_2O)(X)$

Peroxide Oxidation

(L) (**2**)$Fe^{IV}(O)(X) + (CH_3)_3COOH \rightarrow$ (**2**)$Fe^{III}(H_2O)(X) + (CH_3)_3COO^{\bullet} + H^+$

(M) $(CH_3)_3COO^{\bullet} \rightarrow (CH_3)_3CO^{\bullet} + 1/2\,O_2$

(N) $(CH_3)_3CO^{\bullet} \rightarrow (CH_3)_2C{=}O + CH_3^{\bullet}$

[a] Where X = H_2O or OH^-.

nature of the products at high ABTS, the solvent caged reactions B, C, and D have been proposed. Thus, $(CH_3)_2C$=O and CH_3OH are produced from fragmentation of either solvent caged (C) or free $(CH_3)_3CO^{\bullet}$ (F). The formation of *t*-BuO$^{\bullet}$ and $CH_3^{\bullet}$ spin-trapped adducts of 5,5-dimethyl-1-pyrroline *N*-oxide (DMPO) has been observed in the reaction of *t*-BuOOH with (**1**)Fe^{III}-$(H_2O)(X)$.[2d] Formation of CH_3OH is proposed to occur by reaction of $CH_3^{\bullet}$ with (**2**)$Fe^{IV}(O)(X)$ (reactions D and G) or by reaction of $CH_3^{\bullet}$ with (**2**)$Fe^{III}(H_2O)(X)$ (H).[15] Reactions D and G are precedented[16] and amount to the second step of the two-step "rebound mechanism" proposed by Groves[17] for oxygen insertion into C–H bonds by $(porph^{\bullet+})Fe^{IV}(O)(X)$ species. Our inability to detect $(t\text{-BuO})_2$ and C_2H_6 indicates that the bimolecular dimerizations of eqs 21 and 22 are disfavored in comparison to the

$$2(CH_3)_3CO^{\bullet} \rightarrow (t\text{-BuO})_2 \quad (21)$$

$$2CH_3^{\bullet} \rightarrow C_2H_6 \quad (22)$$

unimolecular fragmentation of $(CH_3)_3CO^{\bullet}$ (F) or the reaction of $CH_3^{\bullet}$ with (**2**)$Fe^{IV}(O)(X)$ (G). The reaction of eq 21 is disfavored due to the low steady-state concentrations of *t*-BuO$^{\bullet}$ and the magnitude of the rate constant ($k_r = 1.4 \times 10^6$ s^{-1} in water[14]) for unimolecular fragmentation of *t*-BuO$^{\bullet}$.

The presence of the iron(II) species, formed in reaction H, has been demonstrated by trapping it as its CO adduct. In the absence of O_2 the iron(II) species is consumed by reacting with (**2**)Fe^{IV}-$(O)(X)$ (K). In the presence of O_2 the iron(II) species is oxidized (reactions I and J) to (**2**)$Fe^{IV}(O)(X)$. Thus, in the absence of O_2, (**2**)$Fe^{IV}(O)(X)$ does not accumulate, but, in the presence of O_2, it can be observed. We have shown[2d] that (**1**)$Fe^{II}(H_2O)(X)$ in water reacts with O_2 to yield (**1**)$Fe^{IV}(O)(X)$.

Since $(t\text{-BuO})_2$ cannot be detected as a product but *t*-BuOO$^{\bullet}$ (reaction M) has been shown to be present during the course of

(14) (a) Erben-Russ, M.; Michael, C.; Bors, W.; Saran, M. *J. Phys. Chem.* **1987**, *91*, 2362. (b) Bors, W.; Tait, D.; Micheal, C.; Saran, M.; Erben-Russ, M. *Israel J. Chem.* **1984**, *24*, 17.

(15) Brault, D.; Neta, P. *J. Am. Chem. Soc.* **1981**, *103*, 2705.

(16) (a) Wiberg, K. B.; Foster, G. *J. Am. Chem. Soc.* **1961**, *83*, 423. (b) Brauman, J. I.; Pandell, A. J. *Ibid.* **1970**, *92*, 329. (c) Wiberg, K. B. In *Oxidation in Organic Chemistry*; Wiberg, K. B., Ed.; Academic Press: New York, 1965; p 69. (d) Lorland, J. P, *J. Am. Chem. Soc.* **1974**, *96*, 2867.

(17) (a) Groves, J. T.; McClusky, G. A. *J. Am. Chem. Soc.* **1976**, *98*, 859. (b) Groves, J. T.; Akinbot, O. F.; Avaria, G. E. In *Miscrosomes, Drug Oxidation and Chemical Carcinogensis*; Coon, M. J., Conney, A. H., Estabrook, R. W., Gelboin, H. V., Gillette, J. R., O'Brien, P. J., Eds.; Academic Press: New York, 1980; p 253.

Scheme V

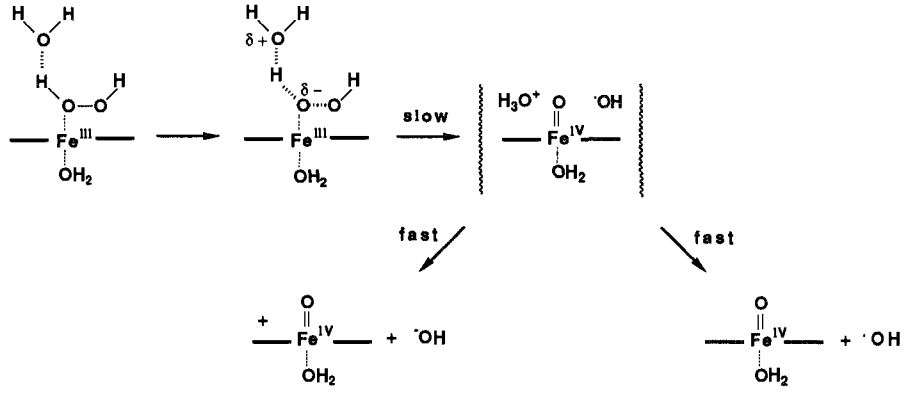

reaction (by DMPO spin trapping[2d]), we have assumed that *t*-BuOO· provides *t*-BuO· without yielding $(t\text{-BuO})_2$ (reaction M). An accepted mechanism for the self-reaction of *t*-BuOO· in solution is shown in eq 23. In the decomposition of the solvent caged

$$2t\text{-BuOO}^{\bullet} \rightarrow [t\text{-BuO}^{\bullet}\ O_2\ t\text{-BuO}^{\bullet}]$$

$$[t\text{-BuO}^{\bullet}\ O_2\ t\text{-BuO}^{\bullet}] \rightarrow (t\text{-BuO})_2 + O_2 \qquad (23)$$

$$[t\text{-BuO}^{\bullet}\ O_2\ t\text{-BuO}^{\bullet}] \rightarrow 2t\text{-BuO}^{\bullet} + O_2$$

species [*t*-BuO· O_2 *t*-BuO·] in organic solvents, the major path (~80%) provides *t*-BuO·.[18] Perhaps this pathway is even more dominant in water. Our spin trap experiments[2d] do not establish the steady-state concentration of *t*-BuOO·. Perhaps the inability to detect $(t\text{-BuO})_2$ and O_2 reflect the relative unimportance of reaction (L).

Epoxide Products: Implications for O–O Bond Cleavage in the Rate-Determining Step. In the reaction of hydrogen peroxide, rate-determining O–O bond homolysis may be followed by $1e^-$ transfer from (**2**)$Fe^{IV}(O)(X)$ to HO· to yield $(2^{+\bullet})Fe^{IV}(O)(X)$ + HO^- (Scheme V).[7] This is much less likely with $Ph(CH_3)_2COOH$ and *t*-BuOOH because the potentials for $1e^-$ oxidation of alkyl-O^- to provide alkyl-O· are about 600 mV less positive than the potential for oxidation of HO^- to HO· (+1.7 V SCE).[4b] No epoxidation can be observed in water (pH ~ 7) by using 1.0 M 3-cyclohexene-1-carboxylate substrate and sufficient hydroperoxide for 700 turnovers of catalyst in experiments with (**1**)$Fe^{III}(H_2O)(X)$ + *t*-BuOOH[2a] and (**2**)$Fe^{III}(H_2O)(X)$ + H_2O_2.[7] These results are in accord with the lack of formation of $(1^{\bullet+})Fe^{IV}(O)(X)$ and $(2^{\bullet+})Fe^{IV}(O)(X)$ species and the known[2a] inability of the iron(IV)-oxo porphyrin (**1**)$Fe^{IV}(O)(X)$ to epoxidize this alkene.

Observations on the Formation of Iron(IV)-Oxo Porphyrin Intermediates. In what follows we shall discuss the various findings with (**2**)$Fe^{III}(H_2O)(X)$ with particular emphasis on the similarities and differences when compared to (**1**)$Fe^{III}(H_2O)(X)$. Reaction of (**2**)$Fe^{III}(X)_2$ with *t*-BuOOH between pH 2.0 and 12, in the presence of O_2, provides observable iron(IV) porphyrin intermediates. In contrast, with (**1**)$Fe^{III}(H_2O)(X)$ and *t*-BuOOH, iron(IV) porphyrin intermediate could be observed only between pH 5.0 and 7.[2a,d] In the case of (**1**)$Fe^{III}(H_2O)(X)$, the disappearance of the iron(IV) species is due, in great measure, to its established[2d] reaction with remaining hydroperoxide and with CH_3· (reactions L and G of Scheme IV). The kinetics for the reaction of alkyl hydroperoxides and hydrogen peroxide with (**1**)$Fe^{IV}(O)(X)$ have been reported.[2d,10] Observation of an iron(IV) species is possible only when its rate of formation is somewhat greater than its rate of disappearance. The (**2**)$Fe^{IV}(O)(X)$ species are much less reactive in the presence of *t*-BuOOH than are the (**1**)$Fe^{IV}(O)(X)$ species. By using a 7-fold excess of *t*-BuOOH, the iron(IV) species generated from (**1**)$Fe^{III}(H_2O)(X)$ (pH 5.0 and 7) is reconverted (with 15% loss) to (**1**)$Fe^{III}(H_2O)(X)$ in a period of several hours. In comparison, in like experiments with (**2**)$Fe^{III}(X)_2$ the iron(IV) species is observable for 100 h (pH 6.3), 80 h (pH 7.25), 50 h (pH 10.37), and 24 h (pH 11.68), and (**2**)$Fe^{III}(H_2O)(X)$ is regenerated with little loss.

The spectrum of the iron(IV) porphyrin intermediate is different when generated at pH 7.25 and at pH 4.87 (Figures 4 and 6, respectively). This suggests an acid dissociation or a change in ligation. The rate of formation and the spectrum of the (**2**)$Fe^{IV}(O)(X)$ species is the same in experiments carried out at pH 7.25 (Figure 4) and pH 10.37 (Figure 5). ABTS titration of the (**2**)$Fe^{IV}(O)(X)$ species generated at pH 7.25 verified it as being $1e^-$ oxidized above the iron(III) state. The spectra at pH 7.25 and 4.87 are much the same as those of the iron(IV)-oxo species produced when employing (**1**)$Fe^{III}(H_2O)(X)$ at pH 6.70 and 5.14, respectively.[2d] The spectrum of (**2**)$Fe^{IV}(O)(X)$ at pH 5.19 is comparable to that observed on spectroelectrochemical controlled potential $1e^-$ oxidation of 5,10,15,20-tetrakis(2,4,6-trimethylphenyl)porphinatoiron(III) hydrate in 5% CH_3OH/CH_2Cl_2 solution.[19]

Upon reaction of *t*-BuOOH with (**2**)$Fe^{III}(H_2O)(X)$ at pH 2.56 there is only seen a very small increase in absorbance in the region of the Soret band of (**2**)$Fe^{III}(H_2O)(X)$ followed by a decrease in the absorbance (Figure 7). The generation of (**2**)$Fe^{IV}(O)(X)$ species can be accomplished, at this low pH, by use of *p*-$NO_2C_6H_4CO_3H$ as an oxidant (Figure 9).

That reaction of *t*-BuOOH with (2)$Fe^{III}(H_2O)(X)$ at pH 7.25 yields (2)$Fe^{II}(H_2O)(X)$ was established by trapping of the latter by carbon monoxide as (**2**)$Fe^{II}(CO)(X)$ in the absence of O_2. The (**2**)$Fe^{II}(CO)(X)$ product was identified by comparing its spectrum with that of authentic (**2**)$Fe^{II}(CO)(X)$. The spectral properties of the authentic (**2**)$Fe^{II}(CO)(X)$ allow the calculation of the percent yield of iron(II) species based upon the initial concentration of iron(III) porphyrin employed. The percentage yields with (**2**)$Fe^{III}(H_2O)(X)$ are ~20% as compared to ~10% previously obtained with (**1**)$Fe^{III}(H_2O)(X)$.[2d] For *t*-BuOOH, the reaction (H) suffices to give an iron(II) species.

Dependence of the Structure of the Oxygen Donor upon the Mechanism of O–O Bond Cleavage. The spectrum of (**1**)$Fe^{IV}(O)(X)$ is detectable on reaction of (**1**)$Fe^{III}(H_2O)(X)$ with *t*-BuOOH and $Ph(CH_3)_2COOH$ only in the presence of O_2.[2d] This is also true when using (**2**)$Fe^{III}(X)_2$. The (**2**)$Fe^{IV}(O)(X)$ does not accumulate in the absence of O_2 due to comproportionation of (**2**)$Fe^{IV}(O)(X)$ + (**2**)$Fe^{II}(H_2O)(X)$ → 2(**2**)$Fe^{III}(H_2O)(X)$ (Scheme IV, (K)). In the presence of O_2, (**2**)$Fe^{II}(H_2O)(X)$ is converted to (**2**)$Fe^{IV}(O)(X)$ (reactions I and J of Scheme IV).

(18) (a) Ingold, K. U. In *Free Radical Vol. I*; Kochi, J. K., Ed.; John Wiley and Sons: New York, 1973; Chapter 2. (b) Howard, J. A. In *Advances in Free Radical Chemistry Vol. 4*; Williams, E. H., Ed.; Academic Press: New York, 1972; Chapter 2.

(19) (a) Calderwood, T. S.; Bruice, T. C. *Inorg. Chem.* **1986**, *25*, 3722. (b) Calderwood, T. S.; Lee, W. A.; Bruice, T. C. *J. Am. Chem. Soc.* **1985**, *107*, 8272. (c) Lee, W. A.; Calderwood, T. S.; Bruice, T. C. *Proc. Natl. Acad. Sci. U.S.A.* **1985**, *82*, 4301.

(20) (a) Walker, F. A.; Balke, V. L.; Mcdermott, G. A. *Inorg. Chem.* **1982**, 3342. (b) Walker, F. A.; Buehler, J.; West, J. T.; Hinds, J. L. *J. Am. Chem. Soc.* **1983**, *105*, 6923. (c) McDermott, G. A.; Walker, F. A. *Inorg. Chim. Acta* **1984**, *91*, 95.

In the reaction of the percarboxylic acids p-$NO_2C_6H_4CO_3H$, m-$ClC_6H_4CO_3H$, and $PhCH_2CO_3H$ and the hydroperoxides $Ph_2(CN)COOH$ and $Ph_2(CO_2CH_3)COOH$ with both (**1**)$Fe^{III}(H_2O)(X)$ and (**2**)$Fe^{III}(H_2O)(X)$, an iron(IV) species is formed in the absence of O_2 (pH 7.25). For the percarboxylic acids, this may be explained through the known heterolytic O–O bond-breaking oxidation being accompanied by a comproportionation reaction (eqs 24a,b) or followed by reduction of the porphyrin iron(IV) π-cation radical by RCO_2H (eqs 24a,c).[2a] That reaction

$$(porph)Fe^{III}(H_2O)(X) + RCO_3H \rightarrow (porph^{\bullet+})Fe^{IV}(O)(X) + X + RCO_2H \quad (24a)$$

$$(porph)Fe^{III}(H_2O)(X) + (porph^{\bullet+})Fe^{IV}(O)(X) \rightarrow 2\,(porph)Fe^{IV}(O)(X) \quad (24b)$$

$$RCO_2H + (porph^{\bullet+})Fe^{IV}(O)(X) \rightarrow RCO_2^{\bullet} + (porph)Fe^{IV}(O)(X) \quad (24c)$$

of (**2**)$Fe^{III}(H_2O)(X)$ with $Ph_2(CN)COOH$ and $Ph_2(CO_2CH_3)COOH$ provides (**2**)$Fe^{IV}(O)(X)$ in the absence of O_2 is in accord with either of two mechanisms. The first is a change of mechanism from homolytic O–O bond breaking with t-BuOOH and $Ph(CH_3)_2COOH$ to heterolytic O–O bond breaking (as in eq 24) with $Ph_2(CN)COOH$ and $Ph_2(CO_2CH_3)COOH$. A second possibility would be that iron(II) species react rapidly with $Ph_2(CN)COOH$ and $Ph_2(CO_2CH_3)COOH$ via a heterolytic mechanism eq 25. The base strengths of $Ph_2(CO_2CH_3)CO^-$ and

$$Ph_2(CN)COOH + (2)Fe^{II}(X)_2 \rightarrow Ph_2(CN)COH + (2)Fe^{IV}(O)(X) \quad (25)$$

$Ph_2(CN)CO^-$ are less than those of t-BuO^- and $Ph(CH_3)CO^-$ but greater than RCO_2^- species. Thus, the oxidizing abilities of $Ph_2(CO_2CH_3)COOH$ and $Ph_2(CN)COOH$ lie midway between alkyl and acyl hydroperoxides. Details of the reaction of $Ph_2(CO_2CH_3)COOH$ and $Ph_2(CN)COOH$ with (**1**)$Fe^{III}(H_2O)(X)$ and (**2**)$Fe^{III}(H_2O)(X)$ will be reported separately.

Hydrogen Peroxide can be considered to be a special case. With or without O_2, reaction of H_2O_2 with (**2**)$Fe^{III}(H_2O)(X)$ or (**1**)$Fe^{III}(H_2O)(X)$ does not result in the observable formation of iron(IV) porphyrin species but in the rapid decomposition of the parent iron(III) porphyrins (Figure 10). Also, it was shown that the iron(IV)-oxo intermediate generated with t-BuOOH disappears on addition of hydrogen peroxide.[2d] In contrast, in reactions with t-BuOOH or $Ph(CH_3)_2COOH$, even under anaerobic conditions, no more than 10% of (**2**)$Fe^{III}(H_2O)(X)$ decomposed (vide supra).

Influence of Electronic Effects in the Tetraphenylporphyrin Moiety. Possibly the most detailed investigation of substituent effect upon the electrophilic character of the central metal ion brought about by meta- and para-substitution of tetraphenylporphyrins has been carried out by Walker's laboratory. Substituent effects have been shown to be nonadditive, and many important aspects have been described.[20] Ortho substitution effects have not been extensively investigated. From this and the previous paper in this journal three pertinent observations may be made. The value of the pK_a for the acid dissociation $(porph)Fe^{III}(H_2O)_2 \rightleftharpoons (porph)Fe^{III}(H_2O)(HO) + H^+$ is larger for (**2**)$Fe^{III}(H_2O)_2$ than for (**1**)$Fe^{III}(H_2O)_2$. This has been explained by a field effect for which there is precedence.[7] The rates and their pH dependence for the reaction of t-BuOOH with (**2**)$Fe^{III}(H_2O)(X)$ and (**1**)$Fe^{III}(H_2O)(X)$ are comparable. The pK_a and kinetic studies suggest that there is little transmission of electronic effects from substituents in the ortho- position of iron(III) tetraphenylporphyrin to the iron(III) moiety. On the other hand, (**2**)$Fe^{IV}(O)(X)$ species are much more stable in solution at all pH values than are (**1**)$Fe^{IV}(O)(X)$ species. Further, the rates of reaction of t-BuOOH with (**1**)$Fe^{IV}(O)(X)$ are greater than are the rates for reaction with (**2**)$Fe^{IV}(O)(X)$.

Acknowledgment. This research was supported by grants from the National Institutes of Health and the National Science Foundation. K.M. expresses gratitude to the National Chemical Laboratory for Industry (Tsukuba, Japan) for his personal support and travel funds from Japan to Santa Barbara.